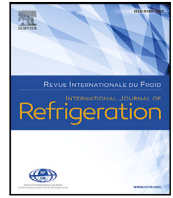




Contents lists available at ScienceDirect

International Journal of Refrigeration

journal homepage: www.elsevier.com/locate/ijrefrig

Analysis of map-based models for reciprocating compressors and optimum selection of rating points

Analyse de modèles basés sur des abaques pour les compresseurs alternatifs et sélection optimale des points d'évaluation

J. Marchante-Avellaneda ^{a,*}, E. Navarro-Peris ^a, J.M. Corberan ^a, Som S. Shrestha ^b

^a Instituto Universitario de Investigación en Ingeniería Energética, Universitat Politècnica de València, Camino de Vera s/n, 46022 Valencia, Spain

^b Buildings and Transportation Science Division, Oak Ridge National Laboratory, One Bethel Valley Road, Oak Ridge, TN, 37831, USA

ARTICLE INFO

Keywords:

AHRI polynomials
Heat pumps
Empirical models
Reciprocating compressors
Energy consumption
Mass flow rate

Mots clés:

Polynômes AHRI
Pompes à chaleur
Modèles empiriques
Compresseurs alternatifs
Consommation énergétique
Débit massique

ABSTRACT

The present work includes an in-depth performance analysis in fixed-speed reciprocating compressors. The industry standard for compressor characterization is the AHRI-540, which uses a 10-term and third-degree polynomial to characterize mass flow rate and energy consumption. However, the suitability of such a high-degree polynomial is unclear, and the potential for overfitting and extrapolation errors cannot be ignored. This work analyzes the response surfaces of mass flow rate and energy consumption in reciprocating compressors to determine if more concise models with lower degrees are more suitable. For that purpose, a massive experimental dataset with multiple compressors using different refrigerant and suction conditions was analyzed to obtain overall conclusions in the compressor field. The results of the present work showed that mass flow rate modeling requires lower-degree polynomials. However, the energy consumption characterization is more complex, and the model reported in the standard may be justified. Additionally, it was found that, if the specific energy consumption is selected as the modeling variable, it is possible to use a compact polynomial expression, which can also be extended to scroll compressors and also has the advantage of reducing the experimental data necessary for the model fit. Finally, by selecting the mass flow rate and the specific energy consumption as response variables, this work also explores other critical issues related to the experimental points' location and minimum sample sizes required in order to minimize the experimental costs and increase the model accuracy.

1. Introduction

Modeling and simulation are widespread and valuable techniques in industrial and research fields. Due to the rapid evolution and calculation power of personal computers, the generation of simulated results is simpler and cheaper compared with experimental testing. It helps to significantly reduce the time and money required when manufacturers or researchers are focused on improving designs to satisfy new environmental regulations or implement new and more efficient control strategies.

Since heat pumps (HPs) play a key role in residential heating and cooling applications, it is essential to accurately characterize their performance by modeling the different components installed in these units. In this sense, one of the main components is the compressor,

which pumps the refrigerant through these units in order to generate the desired heating or cooling effect. As stated by [Chua et al. \(2010\)](#), the progress and enhancement of compressor technologies can cause a drastic decline of up to 80% of the HP electrical energy consumption. For these reasons, much scientific literature focuses on characterizing compressor performance, where two of the most analyzed technologies are scroll and reciprocating compressors, suitable for use in many applications from 100 W up to 100 kW.

The main purpose of compressor models is to provide a mathematical transcription describing how the compressor works in terms of thermodynamic processes inside the compressor shell. These models are typically used to predict compressor performance over the entire working map and can be categorized based on the degree of detail employed in their construction ([Rasmussen and Jakobsen, 2000](#)).

* Corresponding author.

E-mail addresses: jamarav@iie.upv.es (J. Marchante-Avellaneda), emilio.navarro@iie.upv.es (E. Navarro-Peris), energeti@upvnet.upv.es (J.M. Corberan), shresthas@ornl.gov (S.S. Shrestha).

<https://doi.org/10.1016/j.ijrefrig.2023.06.002>

Received 8 February 2023; Received in revised form 1 June 2023; Accepted 4 June 2023

Available online 9 June 2023

0140-7007/© 2023 The Author(s). Published by Elsevier B.V. This is an open access article under the CC BY license (<http://creativecommons.org/licenses/by/4.0/>).

This degree of detail will generally depend on the assumptions and the input information required. For example, theoretical and semi-empirical models require a higher level of understanding of the compressors boundary conditions and the geometry of its internal components, which can, in many cases, only be supplied by the manufacturer. They are based on physical principles or chemical laws and, in the case of semi-empirical models, are completed through experimental data to describe the most complex processes. One of the most common approaches used for simple compressor modeling is to consider the real compression as polytropic (e.g., Popovic and Shapiro, 1995; Mackensen et al., 2002). Then other authors include more detailed models developing them as construction-oriented or phenomena-oriented models, where the compressor is divided into more or fewer control volumes that are linked in terms of mass and energy flows. For example, Corberan et al. (2000) introduce a very detailed model for refrigeration reciprocating compressors, including the dynamics of the valves. Winandy et al. (2002) – according to the approach developed in the ASHRAE toolkit (Bourdouxhe et al., 1994) – develop a phenomena-oriented model including an estimation of the ambient losses for a more accurate prediction of the discharge temperature and considering the compression as isentropic. Navarro et al. (2007) also use a similar approach but with a more detailed analysis, including electromechanical losses and refrigerant leakages effects. The recent paper of Roskosch et al. (2017) also introduces a very detailed model for a reciprocating compressor calculating the piston position as a function of the crank angle and developing it as a set of differential equations for estimating the compressor efficiencies.

Unfortunately, the compression process is extremely complex to permit the use of the abovementioned model typologies without assuming some simplifying assumptions. Moreover, detailed modeling approaches result in models that are difficult to implement and adjust, especially for the common user. In this sense, empirical models allow us to describe processes with a high degree of complexity by using experimental information and regression analysis. They provide more flexibility in predicting compressor performance, and the only requirement is to dispose of enough experimental information to perform a regression adjustment. For instance, the AHRI-540 standard (AHRI 540, 2020) includes a 3rd-degree polynomial with a total of 10 regression coefficients.

Of these two modeling approaches, the use of AHRI polynomials is the most used one by the community to represent the compressor behavior. This results from the fact that if many experimental tests are provided for the entire compressor envelope, these polynomials always obtain lower prediction errors than theoretical and semi-empirical models (Cheung and Wang, 2018). However, the literature does not include a clear justification for using a 3rd-degree polynomial. For example, Shao et al. (2004) reported a polynomial model for rotary compressors by selecting only the first and second-order terms from the original AHRI polynomial with also high accuracy. On the other hand, other authors include polynomial models with more terms for variable-speed compressors, like the reported models by Guth and Atakan (2023), where the authors introduce a polynomial model of 27 terms. However, these models are often presented without a thorough analysis justifying the selection of a specific polynomial and degree. Considering that these models need experimental data for their fitting, it is recommended to analyze the shape of the response surfaces for the characterized variables before fitting the polynomial models. This step is crucial to understand the trends that need to be captured and avoid overfitting the model. Commonly, when proposing a polynomial model, we must consider an adequate degree of the polynomial without exceeding it to describe the characterized response surface. Including a higher degree and non-significant terms results in a greater dependence of the model on the location of the experimental data. This has the consequence that when experimental information is limited, unnecessary overfitting of the model can lead to important extrapolation/interpolation errors when we intend to predict in areas where

no experimental information is available. Therefore, a comprehensive analysis of response surfaces for a wide range of compressors can provide valuable information when considering polynomial models in this field.

Related to empirical models, there are other relevant considerations, such as the optimum number of tests to properly characterize the compressor behavior or where to place these experimental points in the compressor envelope. In this sense, Design of Experiments (DoE) can help minimize experimentation costs and prediction errors in characterizing compressor behavior. Unfortunately, experimental design is not usually addressed in the field of compressors, and there are only a few studies in this area. Considering the compressor envelope shape, some efficient Designs of Experiments methodologies are available in the literature suitable for non-rectangular domains. For example, Aute et al. (2015) and Aute and Martin (2016) propose the Polygonal Design. This methodology combines the manual selection of points – selecting the vertex of the compressor envelope – with cluster design for a specific sample size. Vering et al. (2021) also present an interesting analysis for a fixed-speed scroll compressor, selecting the Optimal Design methodology. This methodology selects the location of test points according to an optimality criterion for a specific polynomial expression. It is suitable only for linear models and easy to implement due to the huge quantity of statistical software with pre-programmed functions.

Against this background, this paper presents a detailed analysis of the polynomial model approach for characterizing reciprocating compressors. The analysis is based on a database from the “*Low-GWP Alternative Refrigerants Evaluation program*”, which provides comprehensive and trustworthy calorimeter data for various compressors and refrigerants. The main objective will be to clarify the best way to characterize compressor performance and to obtain overall conclusions in the compressor field. This database includes a significant amount of scroll and reciprocating compressors from different manufacturers, working with different refrigerants, and a lot of experimental tests located throughout the working range. A previous study (Marchante-Avellaneda et al., 2023) performed an in-depth analysis of the shape and modeling of the response surfaces for the energy consumption and mass flow rate in scroll compressors. It was possible to verify that the AHRI polynomial includes an unnecessary number of terms, being the response surfaces in scroll compressors quite smooth and allowing the use of lower-degree polynomials. Due to the differences in operation between scroll and reciprocating compressors, this study aims to evaluate the type of polynomial models suitable for reciprocating compressors. Preliminary results of the present work for reciprocating compressors were also presented at Marchante-Avellaneda et al. (2022). This paper includes a more detailed analysis performed on a larger number of reciprocating compressors. It focuses on determining the differences between scroll and reciprocating compressors, identifying the optimum polynomial expression, determining the best strategy and number of points to perform the experimental test matrices, and suggesting proper approaches to characterize each compressor design effectively. Finally, a new characterization variable – the specific energy consumption – is also introduced in this work due to the advantages observed when characterizing energy consumption. It allows considering low-degree polynomials compared to the AHRI standard, and it is also suitable to characterize both technologies – scroll and reciprocating – using a general expression and reducing the number of points required for its adjustment.

2. Compressor performance data

As a result of the project “*Low-GWP Alternative Refrigerants Evaluation Program*”, the AHRI institute made public an extensive amount of experimental results of several scroll and reciprocating compressors for different refrigerants, new low-GWP mixtures, and suction conditions. The present paper includes the analysis of all the reciprocating compressors tested in this project. The experimental results has been

collected from following reports: AHRI 17 (Borges Ribeiro and Marchi Di Gennaro, 2013a), AHRI 18 (Borges Ribeiro and Marchi Di Gennaro, 2013b), AHRI 28 (Sedliak, 2013a), AHRI 29 (Sedliak, 2013b), AHRI 30 (Sedliak, 2013c), AHRI 35 (Rajendran and Nicholson, 2014a), AHRI 37 (Rajendran and Nicholson, 2014b), AHRI 49 (Sedliak, 2015a), AHRI 50 (Sedliak, 2015b), AHRI 51 (Boscan and Sanchez, 2015), AHRI 59 (Lenz and Shrestha, 2016), AHRI 64 (Pérouffe and Renevier, 2016a), AHRI 67 (Pérouffe and Renevier, 2016b), AHRI 69 (Pérouffe and Renevier, 2016c).

After analyzing all this experimental information, we have identified two different behaviors for the energy consumption based on the application range:

- Low/Medium evaporating pressure conditions (L/M-BP).
- High values of evaporating pressure (HBP).

Moreover, the collected data include the evaluation of compressor performance for different fluids and suction conditions. Therefore their effect on the performance will also be discussed in this work.

Table 1 briefly summarizes the most important features of the reciprocating compressors analyzed. Based on the number of points, AHRI 30 (L/M-BP compressor) and AHRI 59 (HBP compressor) have been selected as examples to describe how the performance depends on operating conditions. The general conclusions of these two compressors have been confirmed with the other compressors included in Table 1. The results for the rest of the compressors are supplied as supplementary material.

Table 1
Summary of the experimental information collected.

Report	Compressor model	Manufacturer	Displacement cm ³ /rev	Refrigerants tested	Test cond. ^a °C	Test points ^b	Total tests
AHRI 17	NJ7240F	Embraco	34.38	R22/R1270	a	12/12	24
AHRI 18	EG80HLR	Embraco	7.15	R134a/N13a/ARM42a	b	12/8/12	32
AHRI 28	NEK2134GK	Embraco	8.77	R404A/L40	c/a/b	36/36	72
AHRI 29	NEK2134GK	Embraco	8.77	DR7	c/a/b	36	36
AHRI 30	NEK6214Z	Embraco	16.80	R134a/R1234YF	c/a/b	45/45	90
AHRI 35	CS14K6E-TF5	Copeland	47.15	DR7	a/b	52	52
AHRI 37	CS14K6E-TF5	Copeland	47.15	L40	a/b	51	51
AHRI 49	NEK2134GK	Embraco	8.77	R455A	c/a/b	36	36
AHRI 50	NEK2134GK	Embraco	8.77	DR3	c/a/b	36	36
AHRI 51	4GE-23-40P	Bitzer	971.26	R449A/R404A	e	12/12	24
AHRI 59	H84B223ABC	Bristol	30.51	R410A/L41-1/DR5A/ARM71a/D2Y60/R32	a	15/15/15/15/17/15	92
AHRI 64a	FH2511Z	Tecumseh	74.23	R404A/DR7	d/e	28/23	51
AHRI 64b	FH4540Z	Tecumseh	74.23	R404A/DR7	d/e	34/27	61
AHRI 67a	FH2511Z	Tecumseh	74.23	ARM25	d	37	37
AHRI 67b	FH4540Z	Tecumseh	74.23	ARM25	d	16	16
AHRI 69a	FH2511Z	Tecumseh	74.23	ARM20b	d/e	30	30
AHRI 69b	FH4540Z	Tecumseh	74.23	ARM20b	d	16	16

^aSH level or suction temperature: a. *SH* = 11 K ; b. *SH* = 22 K ; c. *T*_s = 18 °C ; d. *SH* = 10 K ; e. *T*_s = 20 °C.

^bTotal experimental tests: 756.

Table 2
New refrigerants composition (Low-GWP HFC mixtures).

Reported name	ASHRAE designation ^{abc}	Company	Refrigerant composition	(% mass)
N13a	–	Honeywell	R134a/R1234yf/R1234ze(E)	42.0/18.0/40.0
ARM42a	≈R516A	Arkema	R134a/R152a/R1234yf	7.0/11.0/82.0
L40	–	Honeywell	R32/R152a/R1234yf/R1234ze(E)	40.0/10.0/20.0/30.0
DR7	R454A	Dupont	R32/R1234yf	36.0/64.0
DR3	R454C	Dupont	R1234yf/R32	78.5/21.5
L41-1	R446A	Honeywell	R32/R1234ze(E)/Butane	68.0/29.0/3.0
DR5A	R454B	Dupont	R32/R1234yf	68.9/31.1
ARM71a	R459A	Arkema	R32/R1234yf/R1234ze(E)	68.0/26.0/6.0
D2Y60	≈R454A	Deikin	R32/R1234yf	40.0/60.0
ARM25	R465A	Arkema	R32/R1234yf/Propane	21.0/71.1/7.9
ARM20b	R457B	Arkema	R32/R1234yf/R152a	35.0/55.0/10.0

^aRefrigerant designation according to ANSI/ASHRAE Standard 34 (2019).

^b–: Development mixture.

^c≈: Development mixture with a similar composition to an ASHRAE-designated mixture.

Finally, Table 2 includes the composition of the new low-GWP mixtures tested. The thermophysical properties were estimated with the Refprop database (Lemmon et al., 2018), considering the condensing and evaporating temperatures at the dew point.

3. Compressor performance analysis

The benefits of using the compressor and volumetric efficiency as a metric for quantifying compressor performance include the advantage that it is a dimensionless parameter that depends less on the size of the compressor or the type of refrigerant examined.

$$\eta_c = \frac{\dot{m}\Delta h_{is}}{\dot{W}_c} \tag{1}$$

$$\eta_v = \frac{\dot{m}}{\rho_{suc}\dot{V}} \tag{2}$$

Moreover, other suitable dimensionless parameters have been suggested as a more reliable way to evaluate compressor performance (see e.g., Pierre (1982) or Navarro-Peris et al. (2013)). Nevertheless, evaluating compressor performance based on efficiencies is more complex than using energy consumption or mass flow rate, as demonstrated in prior research conducted on scroll compressors (Marchante-Avellaneda et al., 2023). The following sections include a qualitative analysis of compressor performance response surfaces. First, the energy consumption parameters are analyzed, followed by the mass flow rate parameters. The efficiencies are introduced first because they are well-known, and they are commonly used parameters showing their disadvantages

if it is intended to obtain models with a high degree of accuracy throughout the working map. Subsequently, the energy consumption and mass flow parameters are analyzed to evaluate the models reported in the AHRI standard. Finally, the analysis of an additional parameter, the specific energy consumption (\dot{W}_c/\dot{m}), is also included in the energy consumption section due to the advantages observed when characterizing both technologies (scroll and reciprocating).

3.1. Compressor consumption analysis

Fig. 1 compares the response surface's shape for the compressor efficiency in a scroll (AHRI 21, the right-hand plot) and a reciprocating (AHRI 30, the left-hand plot) compressor, both at a superheat level of 11 K.

In Fig. 1, the compressor efficiency depends on both variables, evaporating and condensing temperature. The scroll compressor (AHRI

21) shows the zone of maximum efficiency at the highest values of evaporating temperature. On the other hand, the reciprocating compressor (AHRI 30) achieves optimal efficiency when the condensing temperature is highest without having an absolute maximum. Other reciprocating compressors have also been analyzed and obtained similar contour diagrams to that obtained in the AHRI 21. In general, it has been noticed that the response surfaces for the compressor efficiency do not show smooth trends, requiring an empirical model with many parameters.

Another critical aspect related to the characterization of the compressor efficiency or energy consumption is to analyze its dependence on the level of superheat or suction temperature fixed. In this sense, Fig. 2 illustrates how the energy consumption/compressor efficiency change depending on the evaporating temperature/pressure ratio, including the base refrigerant (R134a), two different SH levels, and a constant suction temperature ($SH = 11\text{ K}$, $SH = 22\text{ K}$ and $T_s = 18\text{ }^\circ\text{C}$).

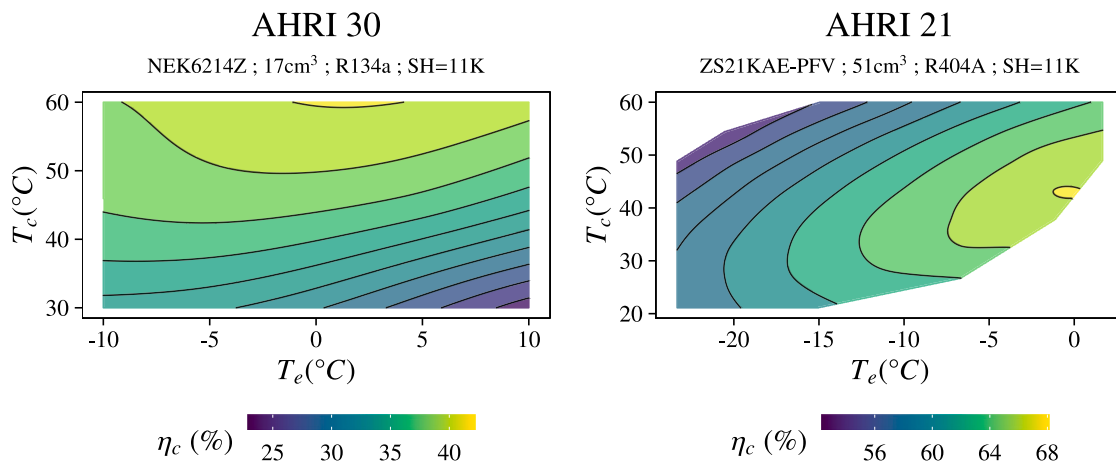


Fig. 1. η_c contour plots of AHRI 21 (scroll, right-hand plot) and AHRI 30 (reciprocating, left-hand plot) with a superheat of 11 K and their base refrigerant.

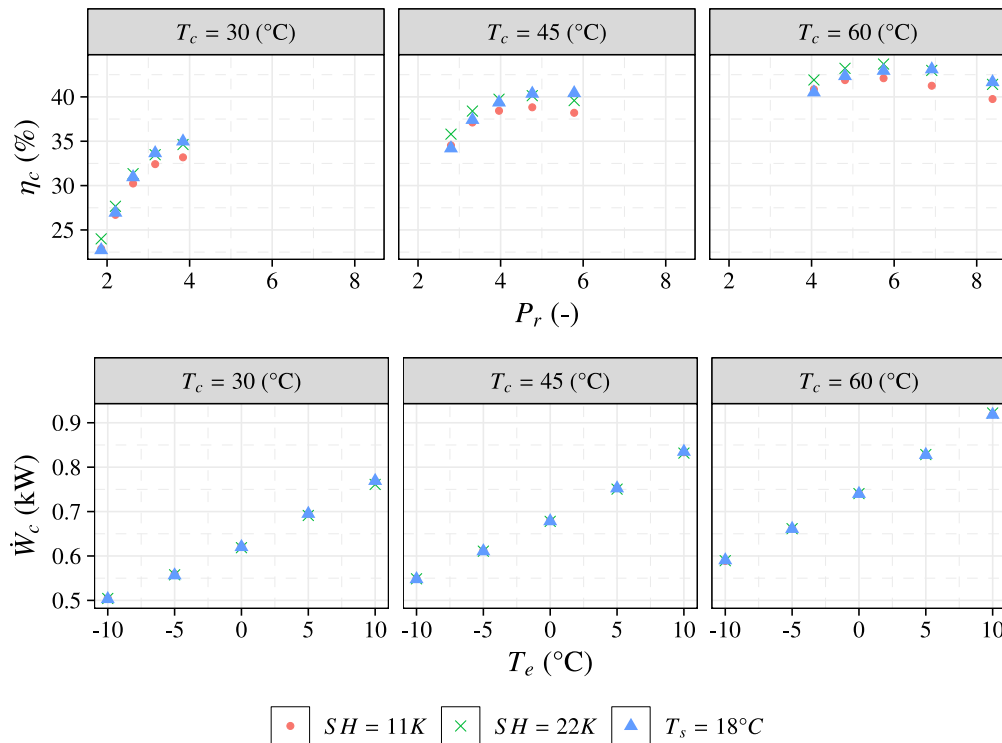


Fig. 2. η_c and \dot{W}_c at different SH and suction temperature (AHRI 30 R134a).

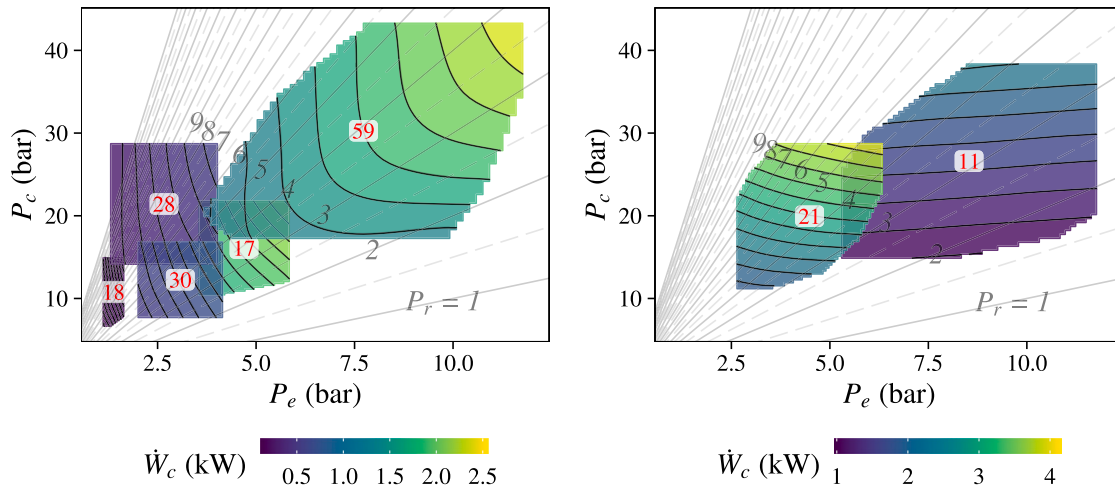


Fig. 3. \dot{W}_c contour plots of AHRI 17, 18, 28, 30, 59 (reciprocating, left-hand plot) and AHRI 11, 21 (scroll, right-hand plot) compressors for their reference refrigerant.

It also includes an additional parameter, the condensing temperature, to performs a matrix of plots for different levels of this variable and simplify the graph visualization.

As illustrated in Fig. 2, the superheat level and the suction temperature affect compressor efficiency but not energy consumption. It can be seen that compressor efficiency tends to increase with a higher superheat level. This result is consistent with prior studies conducted on scroll compressors (Marchante-Avellaneda et al., 2023). At the same time, the energy consumption is directly related to the evaporation temperature, with only a small influence of the condensing temperature (\dot{W}_c rise when T_c increases). This slight dependence on condensation conditions has been identified in the major part of the compressors analyzed. However, according to the trends observed in the compressors included in the AHRI 51 and 59 reports, the condensing temperature significantly affects HBP ranges. To demonstrate this, Fig. 3 displays the contour plots of the energy consumption of various reciprocating compressors (left-hand figure) and scroll compressors (right-hand figure) in terms of condensation and evaporation pressure, including pressure ratio isolines. Labels are used to identify the corresponding AHRI report.

Fig. 3 shows that the reciprocating compressor contour plots display two different trends depending on the evaporation pressure range. For L/M-BP compressors, the energy consumption depends mainly on evaporating pressure with a simple plane as the response surface. As we will see later, this allows us to consider polynomial models with fewer terms. For instance, AHRI 18 and 28 reports (LBP compressor) obtain this simple plane as a function of the evaporation conditions. On the other hand, as the evaporation pressure range increases, the dependence of power consumption on condensation conditions also increases (see MBP compressors AHRI 17 and 30). Lastly, for higher evaporation pressure ranges (HBP compressor), the response surface adopts the second kind of behavior seen, such as the AHRI 59 compressor, where the electrical power consumption mainly depends on both evaporation and condensation conditions. We can therefore intuit that the latter typology will require a more significant number of terms to be included in the polynomial model, including terms dependent on the condensation conditions.

Summing up the trends observed, Fig. 3-left shows that the most significant variable in reciprocating compressors is the evaporation pressure. Then, a secondary dependence on the condensation pressure is also observed in L/M-BP applications, which becomes higher in HBP applications. On the contrary, Fig. 3-right shows that the consumption in scroll compressors depends mainly on the condensation pressure. This different behavior observed between scroll and reciprocating compressors can be attributed to their differences in terms of mass flow rate. Since the electric power consumption in compressors is related to the

pumped mass flow rate, a notable distinction between scroll and reciprocating compressors is the different trends of the volumetric efficiency with the pressure ratio. Contrary to scroll compressors, reciprocating compressors (and piston machines) obtain a considerable drop in volumetric efficiency as the pressure ratio increases due to the existence of a “dead space”. Looking again at Fig. 3, we can see that there is a lower distance between the pressure ratio isolines at lower evaporator pressure ranges. Therefore the electric power consumption maps comprise a wider range of variation for the pressure ratio/mass flow rate, showing only a main dependence on the evaporation pressure.

To conclude the analysis of the energy consumption characterization, an alternative approach to unify the energy consumption behavior, regardless of the operating range and compressor technology, has been developed. Assuming that the differences in the energy consumption behavior are based on the different mass flow trends, an specific energy consumption has been defined as:

$$\dot{W}_{esp} = \frac{\dot{W}_c}{\dot{m}} \tag{3}$$

It is fair to point out that other authors have already undertaken this kind of approach (dividing energy parameter by mass flow parameter). A clear example is shown in Pierre (1982), where the author specifies a correlation for the ratio between volumetric and compressor efficiency (η_v/η_c), instead of directly characterizing the compressor efficiency. This ratio of efficiencies has also been contemplated in this work, but finally, the specific energy consumption was selected because it obtained a more homogeneous behavior, and the response surfaces were easier to characterize. Fig. 4 shows the specific energy consumption maps for the previous compressors analyzed.

It can be seen that the corresponding response surfaces’ shape is non-dependent on the compressor technology. If the specific energy consumption isolines are compared with the pressure ratio isolines, one can see that they intersect, forming a small angle. Thus, different values of the specific energy consumption at a constant pressure ratio are obtained. This is expected since, from Eq. (1), the specific energy consumption is equivalent to the ratio of Δh_{is} and η_c . Therefore, the specific energy consumption is not directly a function of the pressure ratio. However, as the pressure ratio isolines converge to a common vertex at the origin of pressures (0,0), the specific energy consumption isolines also seem to converge at a common vertex. If we consider this last assumption, that allows us to make the following variable change:

$$P'_r = \frac{P_c - z_c}{P_e - z_e} \tag{4}$$

where z_c and z_e are the coordinates of the vertex of the specific energy consumption isolines in the pressure domain. Generally, these

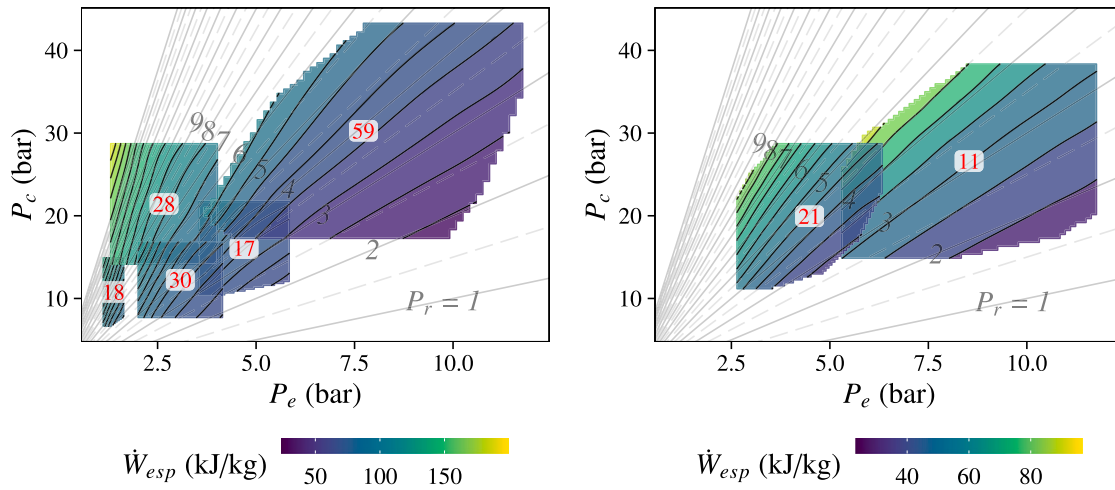


Fig. 4. \dot{W}_{esp} contour plots of AHRI 17, 18, 28, 30, 59 (reciprocating, left-hand plot) and AHRI 11, 21 (scroll, right-hand plot) compressors for their reference refrigerant.

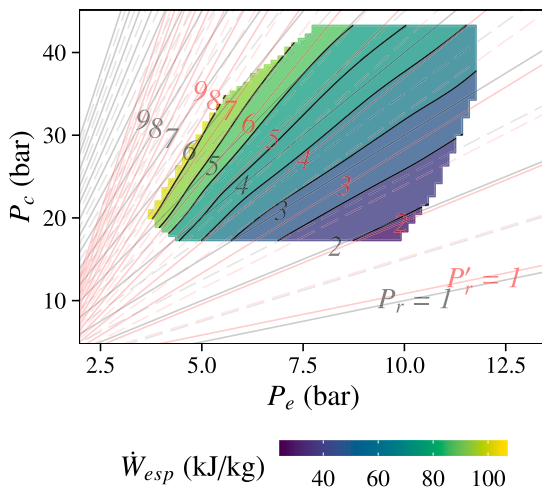


Fig. 5. Specific energy consumption contour plots with the P_r and P'_r isolines of AHRI 59 compressor (reciprocating) and for their reference refrigerant.

coordinates of z_c and z_e will depend on the compressor. Considering appropriate values of z_c and z_e , Fig. 5 represents how the isolines of this new variable (P'_r) are distributed for the AHRI 59 compressor.

Fig. 5 shows how the P'_r isolines correspond with the specific energy consumption isolines. Therefore, we can consider that the specific energy consumption is a function of this new variable:

$$\dot{W}_{esp} = f\left(\frac{P_c - z_c}{P_e - z_e}\right) \tag{5}$$

Finally, Fig. 6 plots how this corrected pressure ratio could characterize the specific energy consumption with a simple polynomial correlation. We can see that the dependence is practically linear or with a slight curvature in some cases. Therefore, the values of z_c and z_e can be obtained simply by proposing a polynomial correlation as a function of P'_r and adjusting by nonlinear regression.

3.2. Mass flow rate analysis

Fig. 7 shows the volumetric efficiency for a reciprocating compressor (AHRI 30, left-plot) and a scroll compressor (AHRI 21, right-plot) working with the reference refrigerant and three suction conditions.

As shown in Fig. 7, the only distinction between both compressors is a clear difference in volumetric efficiency values, which is much lower

for reciprocating compressors. This is so well known due to the strong influence of the “dead space” in piston machines. Both technologies obtain similar trends except for the lower volumetric efficiency values in reciprocating compressors. Volumetric efficiency has a primary linear and negative tendency with pressure ratio – it decreases at higher values of P_r – and it has a secondary dependence on suction conditions. This dependence on suction conditions is commonly rectified by the correction suggested by Dabiri and Rice (1981).

However, although volumetric efficiency is a good parameter to characterize the compressor mass flow rate in general terms, we can see that the relationship with P_r is not strictly linear. There are other second-order dependencies with condensing and evaporating temperatures. Therefore, we can understand why using a polynomial depending on these two variables, as proposed by the AHRI standard, can obtain lower prediction errors to characterize the mass flow rate directly.

In this sense, Fig. 8 represents the mass flow rate maps as a function of evaporating and condensing pressures for the compressors already analyzed in the previous section. The figure shows how the response surfaces for the mass flow rate are practically a plane, and it depends mainly on the evaporation conditions for most scroll and reciprocating compressors. The condensing pressure increases its influence as evaporating pressure increases; this trend can be observed for the AHRI 59 (HBP) compressor. However, the response surfaces remain simple, with smooth changes, compared to those obtained in the previous section for the energy consumption, pointing to the fact that probably, using the third-degree and 10-term polynomial – provided in the AHRI standard – may not be necessary to characterize the mass flow rate.

4. Compressor correlations evaluated

Based on the results obtained in the previous sections, this section includes the analysis of several functionals to characterize reciprocating compressor performance. The proposed functionals consider the complexity of the response surface to be characterized to minimize possible overfitting. Finally, the best correlation for reciprocating compressors based on these polynomials is proposed.

4.1. Correlation for energy consumption

After the first examination of the shape and dependence of the response surface for the energy consumption has been finished, this section explores the most appropriate functional to fit the polynomial model. According to Marchante-Avellaneda et al. (2023), the third-degree and 10-term AHRI polynomial (AHRI 540, 2020) was unnecessary for scroll compressors because the response surfaces were

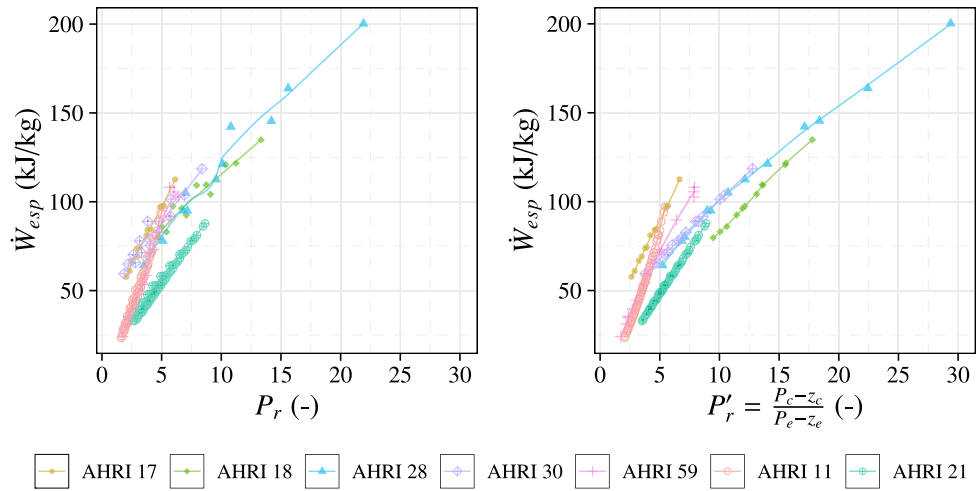


Fig. 6. Specific energy consumption vs. P_r (left-hand plot) and P'_r (right-hand plot) for the AHRI 17, 18, 28, 30 and 59 (reciprocating) and the AHRI 11 and 21 (scroll) compressors for their reference refrigerant.

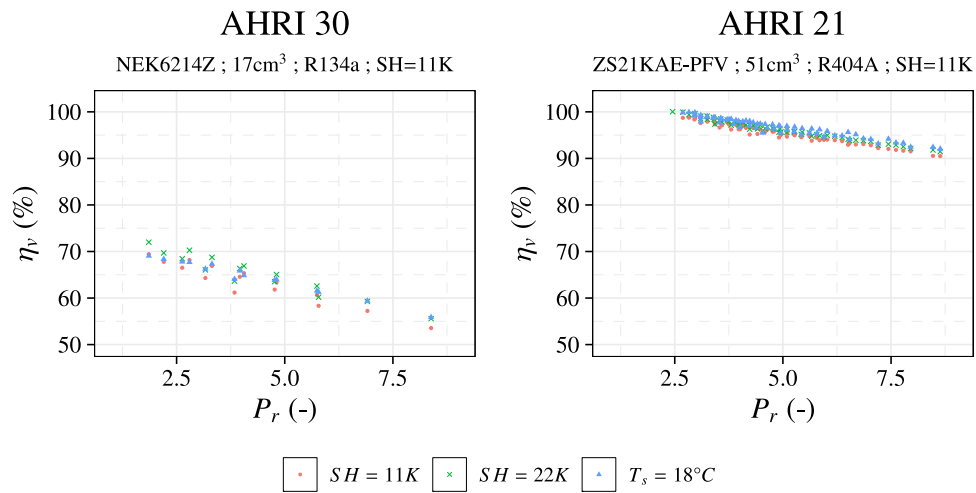


Fig. 7. η_v vs. P_r of AHRI 30 (reciprocating, left-hand plot) and AHRI 21 (scroll, right-hand plot) compressors for their reference refrigerant with a superheat of 11 K.

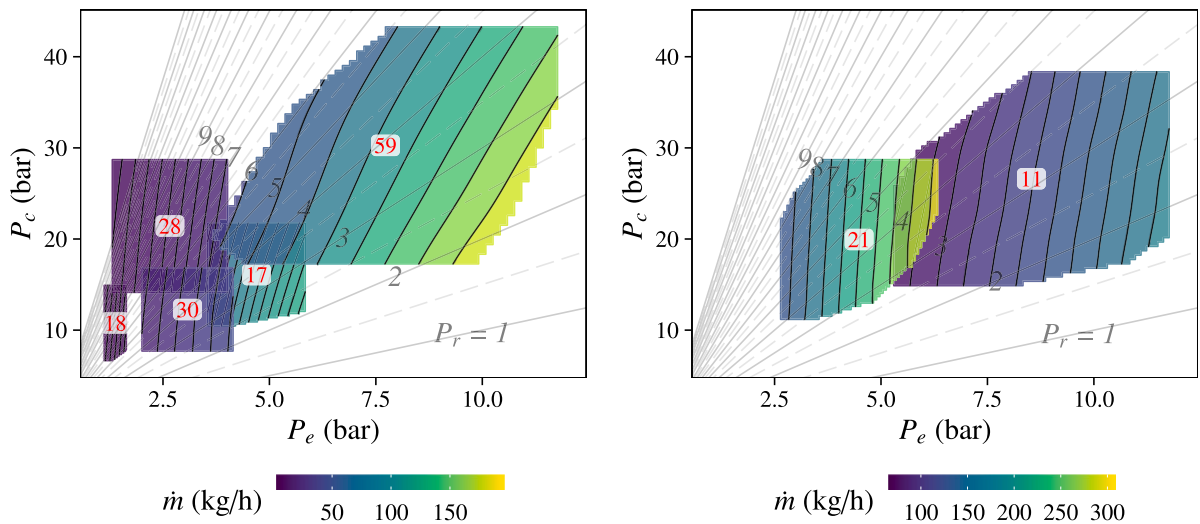



Fig. 8. \dot{m} contour plots of AHRI 17, 18, 28, 30, 59 (reciprocating, left-hand plot) and AHRI 11, 21 (scroll, right-hand plot) compressors for their reference refrigerant.

very smooth with low bending. However, in reciprocating compressors, Fig. 3 has drawn a more complex behavior of the energy consumption as a function of evaporating and condensing conditions that may imply including a greater number of terms in the polynomial overall considering the different compressor behavior observed depending on the evaporating pressure range.

Another important issue in the analysis – which has already been checked for scroll compressors – is the definition of the independent variables. “Should we obtain a polynomial in terms of condensation and evaporation temperature?”, “Is there any advantage of building the model in terms of condensation and evaporation pressure?”.

If the energy consumption of scroll compressors is represented in terms of refrigerant pressure instead of temperature, the response surfaces are more similar to each other. To illustrate this and to check if we get the same effect in reciprocating compressors, Fig. 9 includes a three-dimensional representation of the energy consumption of the AHRI 59 compressor operating at the same SH level and different refrigerants.

Fig. 9 shows the same effect when utilizing a pressure domain for reciprocating compressors. All the refrigerants converge in a single plane, with only a slight variation seen for R32. Therefore, if the pressure domain is selected instead of the temperature domain for the compressor model, the results obtained will be more general in both technologies.

The experimental results have been fitted to the basic correlation proposed by AHRI in terms of temperatures and pressures, expressions (6) and (7). Then additional term reduction methodologies were applied to evaluate the possibility of reducing the number of significant terms in the correlation. In this work, we selected the backward elimination methodology based on the Bayesian information criterion BIC, using the  (Core Team, 2022) statistical software and the additional package RcmdrMisc (Fox, 2022), which includes the `stepwise()` function.

Temperature domain (T)

$$\dot{W}_c = c_0 + c_1 T_e + c_2 T_c + c_3 T_e T_c + c_4 T_e^2 + c_5 T_c^2 + c_6 T_e T_c^2 + c_7 T_e^2 T_c + c_8 T_e^3 + c_9 T_c^3 \quad (6)$$

Pressure domain (P)

$$\dot{W}_c = c_0 + c_1 P_e + c_2 P_c + c_3 P_e P_c + c_4 P_e^2 + c_5 P_c^2 + c_6 P_e P_c^2 + c_7 P_e^2 P_c + c_8 P_e^3 + c_9 P_c^3 \quad (7)$$

Additionally, the energy compressor characterization as a function of the specific energy consumption has been evaluated (Eq. (8)), where P'_r is calculated by Eq. (4).

$$\dot{W}_{esp} = \frac{\dot{W}_c}{\dot{m}_{map}} = k_0 + k_1 P'_r + \dots + k_n P_r^n \quad (8)$$

As shown in Fig. 6, the correction of P_r with the z_c and z_e terms resulted in a practically linear dependence with P'_r and sometimes with a slight curvature. Determining the polynomial degree in Eq. (8) with P'_r has been done iteratively. This means starting with the fit using a linear correlation and increasing the polynomial degree if necessary. The fit can be performed by nonlinear regression to obtain the k_0, \dots, k_n coefficients and the z_c and z_e coordinates. Then, representing the obtained results in a similar way to Fig. 6 with the values of z_c and z_e obtained, it can be seen in a simple way if it is necessary to increase the degree of the polynomial. We must remember that the suction conditions do not affect the energy consumption value, but it fixes the mass flow rate through the compressor. Therefore, the specific energy consumption will also depend on the suction conditions. This means that to convert the specific energy consumption to energy consumption values, we must multiply by the mass flow rate considered in the adjustment of the coefficients k_0, \dots, k_n and z_c, z_e .

Selecting this approach allows the prediction of compressor energy consumption with a quite simple functional of first-degree which depends on only 4 parameters (or 5/6 if we want to increase the prediction accuracy by increasing the degree of the polynomial) and is valid for reciprocating and scroll compressors. This variable could help to represent the compressor energy consumption based on a significantly lower number of experimental tests.

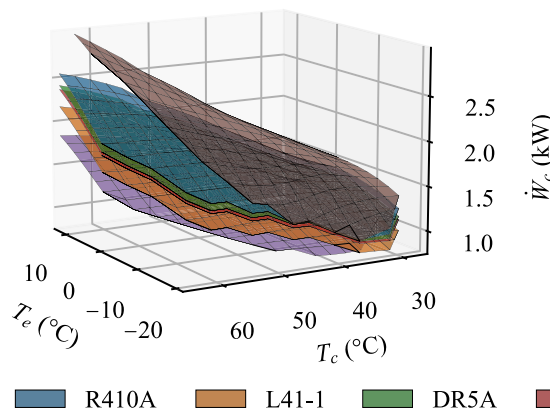
4.2. Correlation for mass flow rate

Summing up the results for the mass flow rate analysis, Fig. 8 shows that the mass flow rate presents more regular surfaces than the energy consumption. The response surface for the mass flow rate in reciprocating compressors is practically a plane depending on the evaporation conditions and with a dependence that can also be important with the condensation conditions. This dependence on the condensation conditions has already been identified for scroll compressors in Marchante-Avellaneda et al. (2023) but in a second-order dependence. However, the mass flow rate response surfaces in reciprocating compressors continue to show reasonably smooth trends. In this sense, a second-order polynomial is adequate and enough in order to obtain low prediction errors. Furthermore, as in the analysis of the mass flow rate for scroll compressors, using pressures as independent variables allows the smoothing of the response surfaces. Therefore, the correlations evaluated by the authors in this study include second-order polynomials evaluated in terms of temperature and pressure (Eqs. (9) and (10)). These functionals, including term elimination methodologies, are also evaluated for the mass flow rate.

2nd order polynomial. Temperature domain (T).

$$\dot{m} = c_0 + c_1 T_e + c_2 T_c + c_3 T_e T_c + c_4 T_e^2 + c_5 T_c^2 \quad (9)$$

a) Temperature domain



a) Pressure domain

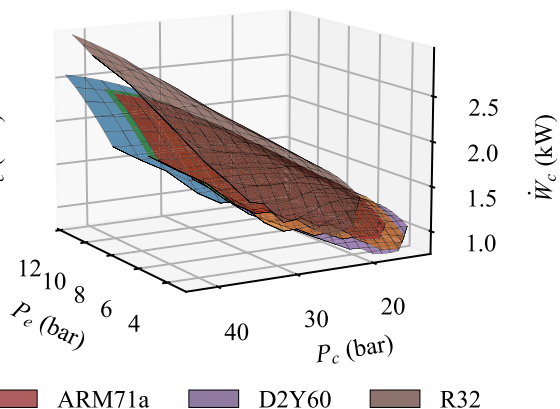


Fig. 9. \dot{W}_c response surfaces as a function of T_c/T_e and vs. P_c/P_e of compressor H84B223ABC (AHRI 59) for 6 different refrigerants.

2nd order polynomial. Pressure domain (P). (10)

$$\dot{m} = c_0 + c_1 P_e + c_2 P_c + c_3 P_e P_c + c_4 P_e^2 + c_5 P_c^2$$

5. Comparison of correlations

5.1. Energy consumption correlations

Tables 3 and 4 display the fitting results for the AHRI 30 and AHRI 59 compressors. The results for the rest of the compressors analyzed are included as supplementary material. AHRI (T) and AHRI (P) models were generated by fitting the original 10-term AHRI polynomial (Eqs. (6) and (7)). AHRI (T-SW) and AHRI (P-SW) models were generated from the original 10-term AHRI polynomial and applied the automated term elimination procedure. These tables list the values of the regression coefficients, including the prediction errors as the **Maximum Relative Error** (MRE, %) and the **Root Mean Square Error** (RMSE, W). The range of the energy consumption values is also included in the last column to determine if the RMSE values are adequate. These errors are also plotted in Fig. 10 to simplify the comparison, including the RMSE as % of the average energy consumption value. The correlations were fitted including all the available experimental points – \dot{W}_c is not impacted by the change of suction conditions – for each refrigerant and compressor. For the specific energy consumption adjustment, the suction conditions considered as \dot{m}_{map} are those used in adjusting the correlation for the mass flow rate included in the following section. The adjustment coefficients k_0, \dots, k_n and z_c and z_e have been adjusted by previously calculating the ratio \dot{W}_c/\dot{m}_{map} , where \dot{m}_{map} is the predicted mass flow rate using Eq. (10). Therefore, the prediction errors for the specific energy consumption include the possible increase in error due to the prediction errors for the mass flow rate. Finally, the corresponding correlations were adjusted to predict the **energy consumption** in kW with **pressure** in bar and **temperatures** in °C and the **specific energy consumption** in kJ/kg with **pressure** in bar.

As we can see from the results for the energy consumption (AHRI (T), AHRI (P), AHRI (T-SW) and AHRI (P-SW) correlations), both temperature-fitted and pressure-fitted models include low prediction errors. For the AHRI 30 (L/M-BP) compressor, the automatic term-elimination procedure results in polynomial models with fewer terms than the AHRI 59 (HBP) compressor. Furthermore, it has been observed that a high degree of collinearity is often found when attempting to fit the 10-term AHRI polynomial to compressors with LBP and MBP

application ranges. For example, when examining the estimated coefficients for the AHRI 30 compressor, it is observed in the AHRI (T) and AHRI (P) models that the regression adjustment is unable to estimate the cubic term (NA) related to condensing conditions (P_c^3 or T_c^3). Then, some regression coefficients show non-significance in the correlation with high *p-values*. This supports the idea that compressors with simpler response surfaces do not require a complex polynomial model, but the best polynomials required for each case are different. Therefore, it is recommended to reduce terms to prevent overfitting when adjusting the model, but it is not possible to supply a suitable general expression for all the compressors and refrigerants. An alternative approach to generating compressor performance maps is to use more advanced tools such as non-parametric regression models, e.g. Thin-Plate-Spline regression model (Green and Silverman, 1993). This method provides a smooth interpolation and produces accurate results, even when the response surface is complex. However, these methodologies reduce the number of non-expert users due to their greater complexity.

On the other hand, we can also observe low prediction errors for the correlation of specific energy consumption, but slightly higher than the previous models. However, we must consider that the previous models have been fitted with a large number of terms and with samples that generally do not exceed 15 experimental points. Therefore, we need to consider the possible extrapolation/interpolation errors that we can obtain when considering models with many terms, as demonstrated in Marchante-Avellaneda et al. (2023). Furthermore, as already shown in the previous sections, selecting \dot{W}_{esp} as the response variable brings some advantages, such as greater simplicity of the response surface (models with fewer terms) and higher similarity between compressor technologies (The same functional can be used to characterize reciprocating or scroll compressors). Thus, for the \dot{W}_{esp} model has been verified that the major part of the analyzed reciprocating compressors gets good results considering a polynomial of degree 3 in Eq. (8). In some cases, a lower degree for the polynomial also has good results, but this is not general. Regarding the significance of the coefficients, it is observed that sometimes one of the two terms, z_c or z_e is non-significant. This means that the coordinates for the vertex of the specific energy consumption isolines can be considered on the coordinate/ordinate axis. However, due to the fact that including both terms (z_c, z_e) does not increase the prediction error, and many of the analyzed compressors obtain significance in both terms, the authors recommend considering both coefficients in the fit in order to obtain a more general correlation. This correlation has also been tested for the scroll compressors analyzed in Marchante-Avellaneda et al. (2023), obtaining similar results to those present in this study. In this case, for

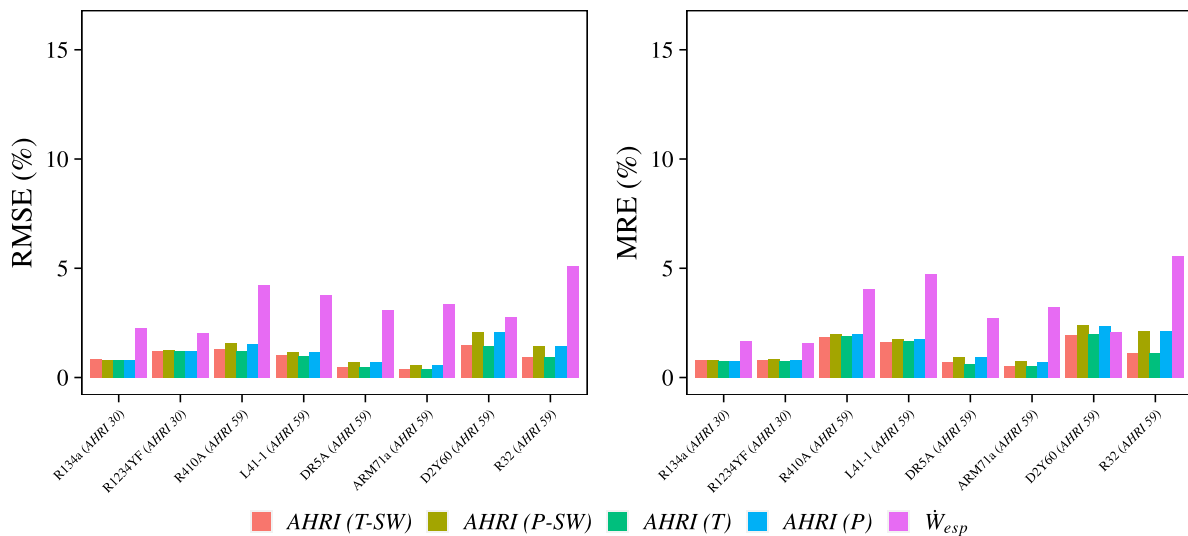


Fig. 10. Energy consumption prediction errors (AHRI 30, 59).

Table 3

Compressor NEK6214Z (AHRI 30). Fitting results for the empirical models of \dot{W}_c in pressure/temperature terms (P)/(T) and by including automatic term elimination methodologies (P-SW)/(T-SW) and fitting results for the empirical model of \dot{W}_{exp} .

	\dot{W}_c (kW) AHRI (T-SW)	MRE (%)	RMSE (W)	\dot{W}_c (kW) AHRI (P-SW)	MRE (%)	RMSE (W)	\dot{W}_c (kW) AHRI (T)	MRE (%)	RMSE (W)	\dot{W}_c (kW) AHRI (P)	MRE (%)	RMSE (W)	\dot{W}_{exp} (kJ/kg)	MRE (%)	RMSE (W)	Fluid \dot{W}_c Range [W] (N ^o tests)
AHRI 30																
c_0, z_c	5.292e-01 (±1.03e-02)***	0.78	1.73	9.481e-02 (±1.42e-02)***	0.78	1.71	5.292e-01 (±1.05e-02)***	0.75	1.67	1.481e-01 (±7.60e-02)***	0.75	1.67	-7.732e+00 (±8.98e-01)***	1.65	4.75	R134a [503, 922] (15/15/15)
c_1, z_c	1.517e-02 (±1.45e-03)***			1.407e-01 (±1.14e-02)***			1.535e-02 (±1.46e-03)***			9.525e-02 (±6.64e-02)**						
c_2, k_0	2.639e-03 (±4.84e-04)***			2.254e-02 (±2.59e-03)***			2.640e-03 (±4.85e-04)***			2.002e-02 (±6.61e-03)***						
c_3, k_1	-1.543e-04 (±6.84e-05)***			-2.438e-03 (±2.93e-03)			-1.543e-04 (±6.82e-05)***			1.138e-03 (±2.74e-03)						
c_4, k_2	1.327e-04 (±1.36e-05)***			-9.158e-04 (±1.77e-04)***			1.338e-04 (±5.15e-05)***			1.059e-02 (±2.08e-02)						
c_5, k_3	1.489e-05 (±5.35e-06)***			2.182e-04 (±5.54e-05)***			1.489e-05 (±5.33e-06)***			-8.479e-04 (±2.41e-04)***						
c_6	2.948e-06 (±7.56e-07)***			2.182e-04 (±5.54e-05)***			2.948e-06 (±7.54e-07)***			1.956e-04 (±7.78e-05)***						
c_7				-3.189e-04 (±2.23e-04)**			-2.540e-08 (±1.10e-06)			-4.119e-04 (±3.16e-04)*						
c_8							-2.022e-06 (±2.67e-06)			-1.290e-03 (±2.21e-03)						
c_9			(NA)	(NA)												
c_0, z_c	5.727e-01 (±1.43e-02)***	0.81	2.33	2.098e-01 (±5.93e-02)***	0.85	2.42	5.727e-01 (±1.46e-02)***	0.77	2.31	1.301e-01 (±1.28e-01)*	0.78	2.33	-9.501e+00 (±1.08e+00)***	1.58	3.94	R1234YF [531, 919] (15/15/15)
c_1, z_c	1.004e-02 (±4.12e-04)***			1.245e-01 (±2.02e-02)***			9.293e-03 (±2.02e-03)***			1.886e-01 (±1.04e-01)***						
c_2, k_0	2.420e-03 (±6.57e-04)***			-2.399e-03 (±9.96e-03)			2.420e-03 (±6.70e-04)***			9.614e-04 (±1.10e-02)						
c_3, k_1	8.642e-05 (±8.84e-06)***			6.421e-03 (±3.00e-03)***			1.226e-04 (±9.42e-05)*			4.268e-03 (±4.26e-03)*						
c_4, k_2	-1.710e-05 (±6.97e-05)			-7.460e-03 (±1.63e-03)***			-1.710e-05 (±7.11e-05)			-2.338e-02 (±3.03e-02)						
c_5, k_3	9.289e-06 (±7.22e-06)*			2.101e-04 (±4.05e-04)			9.289e-06 (±7.37e-06)*			2.101e-04 (±4.02e-04)						
c_6				-1.484e-04 (±1.22e-04)*			-4.015e-07 (±1.04e-06)			-1.484e-04 (±1.21e-04)*						
c_7	2.422e-06 (±1.49e-06)**						2.422e-06 (±1.52e-06)**			3.262e-04 (±4.61e-04)						
c_8							-1.185e-07 (±3.68e-06)			1.216e-03 (±3.01e-03)						
c_9			(NA)	(NA)												

^a+p < 0.1, *p < 0.05, **p < 0.01, ***p < 0.001; Confidence interval of 95% for regression coefficients.

^bTemperatures (K).

^cPressures (bar).

Table 4

Compressor H84B223ABC (AHRI 59). Fitting results for the empirical models of \dot{W}_c in pressure/temperature terms (P)/(T) and by including automatic term elimination methodologies (P-SW)/(T-SW) and fitting results for the empirical model of \dot{W}_{esp} .

	\dot{W}_c (kW) AHRI (T-SW)	MRE (%)	RMSE (W)	\dot{W}_c (kW) AHRI (P-SW)	MRE (%)	RMSE (W)	\dot{W}_c (kW) AHRI (T)	MRE (%)	RMSE (W)	\dot{W}_c (kW) AHRI (P)	MRE (%)	RMSE (W)	\dot{W}_{esp} (kJ/kg)	MRE (%)	RMSE (W)	Fluid \dot{W}_c Range [W] (N° tests)
AHRI 59																
c_0, z_c	8.272e-01 (±5.28e-01)**	1.87	10.80	2.277e-01 (±5.74e-01)	1.97	12.91	8.259e-01 (±7.13e-01)*	1.92	9.86	7.319e-02 (±1.01e+00)	2.01	12.35	2.092e+00 (±4.05e+00)	4.06	34.69	R410A [918, 2552] (15)
c_1, z_e	-4.112e-02 (±5.52e-03)***			3.157e-01 (±1.81e-01)**			-4.476e-02 (±3.13e-02)*			3.260e-01 (±2.26e-01)*			1.259e+00 (±6.84e-01)**			
c_2, k_0	1.176e-02 (±3.83e-02)			-3.486e-02 (±3.77e-02)+			1.279e-02 (±5.39e-02)			-1.998e-02 (±9.05e-02)			-2.115e+00 (±7.02e+00)			
c_3, k_1	1.475e-03 (±1.12e-04)***			1.594e-02 (±4.23e-03)**			1.664e-03 (±1.50e-03)*			1.685e-02 (±7.54e-03)**			1.625e+01 (±2.78e+00)***			
c_4, k_2	-1.168e-03 (±3.61e-04)***			-5.184e-02 (±2.50e-02)**			-1.477e-03 (±1.15e-03)*			-5.502e-02 (±3.48e-02)**			-3.059e-01 (±3.52e-01)+			
c_5, k_3	5.033e-04 (±8.80e-04)			-2.261e-04 (±6.72e-04)			-1.914e-06 (±1.67e-05)			-1.096e-04 (±2.29e-04)						
c_6				-1.221e-04 (±7.30e-05)**			4.708e-04 (±1.28e-03)			-8.609e-04 (±2.97e-03)						
c_7	1.033e-05 (±8.36e-06)*			1.399e-03 (±1.09e-03)*			1.574e-05 (±2.46e-05)			-9.845e-05 (±1.03e-03)						
c_8							-6.609e-06 (±1.75e-05)			1.646e-03 (±2.23e-03)						
c_9	-6.563e-06 (±6.42e-06)*		-6.304e-06 (±9.57e-06)	5.814e-06 (±4.35e-05)												
c_0, z_c	3.903e-01 (±1.21e-01)***	1.64	7.04	-1.029e-01 (±6.01e-01)	1.78	8.23	4.616e-01 (±5.02e-01)+	1.65	6.94	-1.029e-01 (±6.01e-01)	1.78	8.23	1.134e+00 (±3.55e+00)	4.72	26.43	L41-1 [779, 2173] (15)
c_1, z_e	-4.238e-02 (±1.56e-02)***			1.208e-01 (±1.71e-01)			-4.044e-02 (±2.20e-02)**			1.208e-01 (±1.71e-01)			1.193e+00 (±3.36e-01)***			
c_2, k_0	3.906e-02 (±5.42e-03)**			5.558e-02 (±6.59e-02)+			3.353e-02 (±3.80e-02)+			5.558e-02 (±6.59e-02)+			-1.935e+01 (±3.27e+01)			
c_3, k_1	1.940e-03 (±7.44e-04)***			1.082e-02 (±6.88e-03)**			1.846e-03 (±1.06e-03)**			1.082e-02 (±6.88e-03)**			3.298e+01 (±1.79e+01)**			
c_4, k_2	-2.378e-03 (±6.23e-04)***			-1.248e-02 (±3.63e-02)			-2.320e-03 (±8.08e-04)***			-1.248e-02 (±3.34e-02)			-3.247e+00 (±3.41e+00)+			
c_5, k_3	-3.194e-04 (±5.69e-05)**			-3.082e-03 (±2.61e-03)*			-1.866e-04 (±9.02e-04)			-3.082e-03 (±2.61e-03)*			1.827e-01 (±2.07e-01)+			
c_6	-7.662e-06 (±8.26e-06)+			-3.569e-04 (±2.54e-04)*			-6.608e-06 (±1.18e-05)			-3.569e-04 (±2.54e-04)*						
c_7	3.675e-05 (±1.28e-05)**			1.275e-03 (±1.20e-03)*			3.537e-05 (±1.73e-05)**			1.275e-03 (±1.20e-03)*						
c_8	-3.144e-05 (±1.06e-05)***			-2.038e-03 (±2.72e-03)			-3.106e-05 (±1.23e-05)**			-2.038e-03 (±2.72e-03)						
c_9		5.484e-05 (±4.61e-05)**	-9.946e-07 (±6.74e-06)	5.484e-05 (±4.61e-05)**												
c_0, z_c	6.378e-01 (±2.12e-01)***	0.73	3.83	-2.728e-01 (±4.45e-01)	0.96	5.56	6.057e-01 (±2.66e-01)**	0.63	3.68	-2.728e-01 (±4.45e-01)	0.96	5.56	5.346e-01 (±2.77e+00)	2.72	23.63	DR5A [884, 2416] (15)
c_1, z_e	-3.622e-02 (±2.19e-03)***			2.738e-01 (±1.10e-01)**			-3.914e-02 (±1.17e-02)***			2.738e-01 (±1.10e-01)**			1.138e+00 (±4.02e-01)***			
c_2, k_0	2.351e-02 (±1.54e-02)**			3.476e-02 (±4.34e-02)+			2.627e-02 (±2.01e-02)*			3.476e-02 (±4.34e-02)+			-2.314e+01 (±2.11e+01)**			
c_3, k_1	1.366e-03 (±4.75e-05)**			1.288e-02 (±3.99e-03)**			1.508e-03 (±5.59e-04)***			1.288e-02 (±3.99e-03)**			3.359e+01 (±1.24e+01)**			
c_4, k_2	-1.770e-03 (±2.33e-04)***			-4.188e-02 (±4.28e-02)**			-1.857e-03 (±4.82e-04)***			-4.188e-02 (±4.28e-02)**			-3.487e+00 (±2.56e+00)**			
c_5, k_3	1.739e-04 (±3.52e-04)			-2.207e-03 (±1.54e-03)*			1.031e-04 (±4.78e-04)			-2.207e-03 (±1.54e-03)*			2.054e-01 (±1.71e-01)*			
c_6				-1.607e-04 (±1.31e-04)*			-1.594e-06 (±6.24e-06)			-1.607e-04 (±1.31e-04)*						
c_7	2.290e-05 (±4.30e-06)***			3.376e-04 (±5.96e-04)			2.491e-05 (±9.18e-06)***			3.376e-04 (±5.96e-04)						
c_8	-1.481e-05 (±5.09e-06)***			6.263e-04 (±1.30e-03)			-1.566e-05 (±6.52e-06)**			6.263e-04 (±1.30e-03)						
c_9	-3.968e-06 (±2.57e-06)**	2.512e-05 (±2.45e-05)*	-3.416e-06 (±3.57e-06)+	2.512e-05 (±2.45e-05)*												
c_0, z_c	6.062e-01 (±2.21e-01)***	0.53	3.05	-1.965e-01 (±2.87e-01)	0.76	4.25	6.062e-01 (±2.21e-01)***	0.53	3.05	-1.946e-01 (±3.34e-01)	0.73	4.25	1.126e+00 (±2.48e+00)	3.23	25.45	ARM71a [866, 2371] (15)
c_1, z_e	-3.960e-02 (±3.70e-03)***			2.343e-01 (±5.51e-02)***			-3.960e-02 (±3.70e-03)***			2.322e-01 (±8.53e-02)**			1.180e+00 (±3.51e-01)***			
c_2, k_0	2.614e-02 (±1.67e-02)**			3.609e-02 (±2.83e-02)*			2.614e-02 (±1.67e-02)**			3.636e-02 (±3.34e-02)*			-2.169e+01 (±1.95e+01)*			
c_3, k_1	1.617e-03 (±4.64e-04)***			1.166e-02 (±2.06e-03)**			1.617e-03 (±4.64e-04)***			1.159e-02 (±3.15e-03)**			3.380e+01 (±1.15e+01)***			
c_4, k_2	-2.016e-03 (±3.55e-04)***			-3.376e-02 (±5.96e-03)***			-2.016e-03 (±3.55e-04)***			-3.329e-02 (±1.48e-02)**			-3.635e+00 (±2.37e+00)**			
c_5, k_3	6.141e-05 (±3.97e-04)			-2.154e-03 (±1.05e-03)**			6.141e-05 (±3.97e-04)			-2.157e-03 (±1.21e-03)**			2.160e-01 (±1.58e-01)**			
c_6	-3.325e-06 (±5.18e-06)			-2.006e-04 (±7.07e-05)***			-3.325e-06 (±5.18e-06)			-2.031e-04 (±1.06e-04)**						
c_7	2.839e-05 (±7.62e-06)***			5.608e-04 (±2.60e-04)***			2.839e-05 (±7.62e-06)***			5.747e-04 (±4.86e-04)*						
c_8	-2.067e-05 (±5.41e-06)***			-2.067e-05 (±5.41e-06)***			-2.067e-05 (±5.41e-06)***			-3.868e-05 (±1.07e-03)						
c_9	-2.881e-06 (±2.96e-06)+	2.887e-05 (±1.59e-05)**	-2.881e-06 (±2.96e-06)+	2.914e-05 (±1.98e-05)*												
c_0, z_c	5.652e-01 (±1.11e-01)***	1.93	7.79	1.719e-01 (±7.66e-01)	2.41	11.03	6.993e-01 (±4.56e-01)**	2.00	7.51	1.885e-01 (±9.19e-01)	2.35	11.03	-2.173e+00 (±2.70e+00)	2.08	14.61	D2Y60 [787, 1838] (17)
c_1, z_e	-6.267e-02 (±1.43e-02)***			3.368e-01 (±1.84e-01)**			-5.921e-02 (±1.89e-02)***			3.264e-01 (±3.10e-01)*			9.097e-01 (±3.55e-01)***			
c_2, k_0	2.706e-02 (±5.13e-03)***			-3.258e-02 (±7.74e-02)			1.666e-02 (±3.46e-02)			-3.222e-02 (±8.52e-02)			-3.296e+01 (±1.93e+01)**			
c_3, k_1	2.985e-03 (±6.94e-04)***			1.644e-02 (±7.58e-03)**			2.813e-03 (±9.26e-04)***			1.624e-02 (±9.42e-03)**			3.338e+01 (±9.42e+00)***			
c_4, k_2	-2.241e-03 (±5.75e-04)***			-5.908e-02 (±2.10e-02)***			-2.113e-03 (±7.39e-04)***			-5.677e-02 (±5.70e-02)+			-4.097e+00 (±1.66e+00)***			
c_5, k_3	-2.238e-04 (±5.50e-05)**			-2.635e-04 (±3.23e-03)			2.561e-05 (±8.21e-04)			-2.671e-04 (±3.54e-03)			2.327e-01 (±9.82e-02)**			
c_6	-2.244e-05 (±7.65e-06)***			-6.326e-04 (±2.48e-04)***			-2.049e-05 (±1.03e-05)**			-6.445e-04 (±3.81e-04)**						
c_7	3.761e-05 (±1.16e-05)**			1.728e-03 (±1.05e-03)**			3.467e-05 (±1.56e-05)**			1.788e-03 (±1.78e-03)*						
c_8	-2.007e-05 (±1.35e-05)**						-1.879e-05 (±1.48e-05)*			-2.030e-04 (±4.58e-03)						
c_9		4.260e-05 (±5.77e-05)	-1.864e-06 (±6.12e-06)	4.380e-05 (±6.88e-05)												
c_0, z_c	1.682e+00 (±1.81e+00)+	1.11	9.94	3.755e-01 (±1.29e+00)	2.13	15.22	1.682e+00 (±1.81e+00)+	1.11	9.94	3.750e-01 (±1.48e+00)	2.11	15.22	6.101e+00 (±2.70e+00)***	5.57	54.65	R32 [946, 3083] (15)
c_1, z_e	6.653e-02 (±1.03e-01)			2.646e-01 (±2.35e-01)*			6.653e-02 (±1.03e-01)			2.663e-01 (±3.17e-01)+			2.041e+00 (±5.26e-01)***			
c_2, k_0	-5.384e-02 (±1.34e-01)			-2.654e-02 (±1.07e-01)			-5.384e-02 (±1.34e-01)			-2.699e-02 (±1.31e-01)			-1.118e+01 (±3.08e+01)			
c_3, k_1	-4.311e-03 (±4.90e-03)+			3.930e-02 (±1.14e-02)**			-4.311e-03 (±4.90e-03)+			3.908e-02 (±2.52e-02)*			3.532e+01 (±2.05e+01)**			
c_4, k_2	2.181e-03 (±2.43e-03)+			-8.266e-02 (±2.94e-02)***			2.181e-03 (±2.43e-03)+			-8.255e-02 (±3.56e-02)**			-2.589e+00 (±4.39e+00)			
c_5, k_3	2.350e-03 (±3.19e-03)			-3.992e-03 (±2.71e-03)*			2.350e-03 (±3.19e-03)			-3.940e-03 (±6.00e-03)			1.207e-01 (±2.96e-01)			
c_6	7.572e-05 (±5.66e-05)*			2.858e-04 (±2.51e-04)*			7.572e-05 (±5.66e-05)*			2.957e-04 (±1.02e-03)						
c_7	-8.098e-05 (±5.18e-05)*			-2.451e-03 (±9.79e-04)***			-8.098e-05 (±5.18e-05)*			-2.469e-03 (±2.19e-03)*						
c_8	2.706e-05 (±2.59e-05)**			4.892e-03 (±1.84e-03)***			2.706e-05 (±2.59e-05)**			4.908e-03 (±2.66e-03)**						
c_9	-2.169e-05 (±2.47e-05)+		-2.169e-05 (±2.47e-05)+	-1.643e-06 (±1.63e-04)												

^a+p < 0.1, *p < 0.05, **p < 0.01, ***p < 0.001; Confidence interval of 95% for regression coefficients.

^bTemperatures (K).

^cPressures (bar).

scroll compressors, a degree 2 in Eq. (8) is enough to obtain a low prediction error, and a linear correlation can be considered in many of the scroll compressors analyzed in Marchante-Avellaneda et al. (2023). Therefore, the specific energy consumption can be characterized using a simple functional with fewer terms. In addition, this type of correlation has the advantage of non using any statistical methodology of term elimination in order to obtain an expression for all the compressors. The response surfaces analyzed are quite similar regardless of the operating range or compressor technology used.

Finally, to summarize the results, this section includes several models in terms of temperature or pressure capable of accurately characterizing the energy consumption in reciprocating compressors. Similar prediction errors are obtained by fitting the model in terms of pressures or temperatures. However, as mentioned above, defining the model in terms of pressures results in less dependence on the refrigerant used. In addition, using pressures allows for obtaining a more general approach to characterize compressors, including compressors in transcritical cycles, where the condensing pressure remains constant.

5.2. Mass flow rate correlations

Tables 5 and 6 show the fitting results for the AHRI 30 and AHRI 59 compressors. The results for the rest of the compressors analyzed are included as supplementary material. These tables contain the same information as those already analyzed for the energy consumption in the previous section, including the second-order polynomial models in terms of temperature and pressure (2nd order polynomial (T) and (P)), and the same correlations after applying the automatic term elimination methodology (2nd order polynomial (T-SW) and (P-SW)). Fig. 11 also represents the error values of RMSE and MRE, including the RMSE as % of the average mass flow value. These correlations have been obtained by selecting one of the available suction conditions for each compressor analyzed. The results have also been checked by adjusting the proposed functionals to the rest of the suction conditions with similar results. The coefficients are meant to provide the mass flow rate in kg/h with temperatures in °C and pressure in bar.

As seen in the summary tables, a second-order polynomial is enough for characterizing the mass flow rate instead of using the full functional defined in the AHRI standard. The elimination of cubic terms makes it possible to obtain more compact polynomials with a better predictive behavior avoiding overfitting problems with the AHRI polynomials. Nevertheless, most compressors obtain even more compact models by applying the automatic term elimination methodology. Moreover, in most of the compressors analyzed, the functionals with pressures tend to obtain more compact models when applying the automatic term

elimination methodologies. These results agree with the conclusions obtained in Marchante-Avellaneda et al. (2023) for scroll compressors, where selecting pressures as independent variables allowed smoothing and linearization of the mass flow response surface. However, the polynomials in scroll compressors included a lower number of coefficients. Low prediction errors could be obtained by fitting a linear correlation and improving the results by adding an interaction term ($P_c \times P_e$). In reciprocating compressors, these functionals were only suitable for some compressors. Therefore, in general, using Eqs. (9) and (10) to characterize the mass flow rate in reciprocating compressors will be recommended. Furthermore, it will be more suitable to use the correlation in terms of pressure (Eq. (10)) and the automatic term elimination. This results in more compact polynomials and brings up the possibility of characterizing compressors in transcritical cycles.

6. Experimental points required

Once the models proposed in this work to characterize reciprocating compressors have been analyzed, we will focus on selecting proper experimental samples for their adjustment. This topic is addressed in the field of regression modeling by the so-called Design of Experiments methodologies. Commonly, the Design of Experiments tools available in the literature allows us to set the required number of tests, including their location in the experimental domain. The main objective will be to obtain a sample as compact as possible, reducing the experimental costs but simultaneously containing as much information as possible, i.e., with statistical inference. This challenge of selecting a proper sample to obtain a statistically significant sample is not included in the current standard (AHRI 540, 2020), so a focused analysis of this topic is of special relevance and greatly enriches the results obtained in this work.

Focusing on the Design of Experiments methodologies, these techniques can be divided into classical experimental designs and computer-aided designs. The first group defines experimental designs for mainly orthogonal domains, while the second one presents the advantage of defining designs for irregular domains. In the case of compressors, they have two areas of no operation, one limited by the high discharge temperatures, where the integrity of the compressor would be compromised, and another area limited by a low-pressure ratio with a considerable loss of efficiency. Therefore, computer-aided designs are more suitable for compressor applications. These tools have already been analyzed in a previous work focused on scroll compressor characterization (Marchante-Avellaneda et al., 2023), selecting the optimal designs as the most appropriate ones. However, the reciprocating compressor tests analyzed in this work do not include any fine-meshed

Table 5

Compressor NEK6214Z (AHRI 30) with a superheat of 11 K. Fitting results for the empirical models of \dot{m} in pressure/temperature terms (P)/(T) and by including automatic term elimination methodologies (P-SW)/(T-SW).

	\dot{m} (kg/h) 2nd order polynomial (T-SW)	MRE (%)	RMSE (kg/h)	\dot{m} (kg/h) 2nd order polynomial (P-SW)	MRE (%)	RMSE (kg/h)	\dot{m} (kg/h) 2nd order polynomial (T)	MRE ^d (%)	RMSE ^d (kg/h)	\dot{m} (kg/h) 2nd order polynomial (P)	MRE ^d (%)	RMSE ^d (kg/h)	Fluid \dot{m} Range [kg/h] (N° tests)
AHRI 30													
c_0	3.048e+01 (±1.13e+00)***	0.66	0.09	-4.131e+00 (±1.17e+00)***	0.66	0.09	3.048e+01 (±1.21e+00)***	0.65 (0.45)	0.09 (0.07)	-4.598e+00 (±1.80e+00)***	0.69 (0.45)	0.09 (0.07)	R134a [18, 46] (15)
c_1	1.301e+00 (±8.84e-03)***			1.284e+01 (±7.91e-01)***			1.302e+00 (±3.60e-02)***			1.286e+01 (±9.00e-01)***			
c_2	1.104e-01 (±5.33e-02)***			1.104e-01 (±5.70e-02)**			1.104e-01 (±1.85e-01)			7.743e-02 (±1.85e-01)			
c_3													
c_4	1.678e-02 (±1.49e-03)***			-1.097e-01 (±1.28e-01)+			-2.000e-05 (±7.72e-04)			-1.455e-03 (±2.33e-02)			
c_5	-2.222e-03 (±5.89e-04)***	-1.208e-02 (±6.57e-04)***	-1.678e-02 (±1.60e-03)***	-1.097e-01 (±1.38e-01)									
c_6			-2.222e-03 (±6.31e-04)***	-1.501e-02 (±6.90e-03)***									
AHRI 59													
c_0	3.757e+01 (±4.76e+00)***	2.18	0.35	1.871e+00 (±4.14e+00)	2.19	0.41	3.757e+01 (±4.76e+00)***	2.18 (1.94)	0.35 (0.34)	-3.628e+00 (±8.08e+00)	2.20 (1.85)	0.35 (0.33)	R1234YF [24, 55] (15)
c_1	1.334e+00 (±1.42e-01)***			1.245e+01 (±1.25e+00)***			1.334e+00 (±1.42e-01)***			1.445e+01 (±3.77e+00)***			
c_2	1.118e-01 (±2.24e-01)			-5.278e-01 (±3.33e-01)**			1.118e-01 (±2.24e-01)			-1.034e-01 (±8.23e-01)			
c_3	2.440e-03 (±3.04e-03)			7.869e-02 (±1.00e-01)			2.440e-03 (±3.04e-03)			7.869e-02 (±9.78e-02)			
c_4	1.479e-02 (±6.28e-03)***						1.479e-02 (±6.28e-03)***			-3.030e-01 (±5.41e-01)			
c_5	-2.102e-03 (±2.48e-03)+		-2.102e-03 (±2.48e-03)+	-1.736e-02 (±3.09e-02)									

^a+p < 0.1, *p < 0.05, **p < 0.01, ***p < 0.001; Confidence interval of 95% for regression coefficients.

^bTemperatures (K).

^cPressures (bar).

^dThe values in brackets are the errors for the full AHRI polynomial (Temperature and pressure domain).

Table 6

Compressor H84B223ABC (AHRI 59) with a superheat of 11 K. Fitting results for the empirical models of \dot{m} in pressure/temperature terms (P)/(T) and by including automatic term elimination methodologies (P-SW)/(T-SW).

	\dot{m} (kg/h) 2nd order polynomial (T-SW)	MRE (%)	RMSE (kg/h)	\dot{m} (kg/h) 2nd order polynomial (P-SW)	MRE (%)	RMSE (kg/h)	\dot{m} (kg/h) 2nd order polynomial (T)	MRE ^d (%)	RMSE ^d (kg/h)	\dot{m} (kg/h) 2nd order polynomial (P)	MRE ^d (%)	RMSE ^d (kg/h)	Fluid \dot{m} Range [kg/h] (N° tests)
AHRI 59													
c_0	1.777e+02 ($\pm 1.15e+01$)***			-2.200e+01 ($\pm 1.20e+01$)**			1.777e+02 ($\pm 1.15e+01$)***			-2.041e+01 ($\pm 1.39e+01$)**			R410A [31, 196] (15)
c_1	7.194e+00 ($\pm 4.54e-01$)***	5.41	1.10	2.770e+01 ($\pm 1.15e+00$)***	6.04	1.18	7.194e+00 ($\pm 4.54e-01$)***	5.41 (2.99)	1.10 (0.56)	2.710e+01 ($\pm 2.51e+00$)***	5.66 (2.43)	1.15 (0.5)	
c_2	-9.504e-01 ($\pm 5.47e-01$)**			-1.885e+00 ($\pm 7.50e-01$)***			-9.504e-01 ($\pm 5.47e-01$)**			-1.867e+00 ($\pm 7.90e-01$)***			
c_3	-3.083e-02 ($\pm 9.40e-03$)***			-1.798e-01 ($\pm 4.20e-02$)***			-3.083e-02 ($\pm 9.40e-03$)***			-1.924e-01 ($\pm 6.39e-02$)***			
c_4	6.819e-02 ($\pm 1.09e-02$)***						6.819e-02 ($\pm 1.09e-02$)***			6.013e-02 ($\pm 2.21e-01$)			
c_5	-8.085e-03 ($\pm 6.04e-03$)*			1.380e-02 ($\pm 1.29e-02$)*			-8.085e-03 ($\pm 6.04e-03$)*			1.528e-02 ($\pm 1.46e-02$)*			
c_0	1.112e+02 ($\pm 9.50e+00$)***	4.32	0.91	-1.340e+01 ($\pm 1.45e+01$)+	9.08	1.29	1.112e+02 ($\pm 9.50e+00$)***	4.32 (3.71)	0.91 (0.45)	-1.340e+01 ($\pm 1.45e+01$)+	9.08 (4.56)	1.29 (0.72)	L41-1 [17, 126] (15)
c_1	5.180e+00 ($\pm 3.77e-01$)***			1.992e+01 ($\pm 3.30e+00$)***			5.180e+00 ($\pm 3.77e-01$)***			1.992e+01 ($\pm 3.30e+00$)***			
c_2	-7.081e-01 ($\pm 4.54e-01$)**			-1.265e+00 ($\pm 1.00e+00$)*			-7.081e-01 ($\pm 4.54e-01$)**			-1.265e+00 ($\pm 1.00e+00$)*			
c_3	-2.792e-02 ($\pm 7.80e-03$)***			-2.369e-01 ($\pm 1.02e-01$)***			-2.792e-02 ($\pm 7.80e-03$)***			-2.369e-01 ($\pm 1.02e-01$)***			
c_4	5.887e-02 ($\pm 9.04e-03$)***			3.145e-01 ($\pm 3.70e-01$)+			5.887e-02 ($\pm 9.04e-03$)***			3.145e-01 ($\pm 3.70e-01$)+			
c_5	-3.810e-03 ($\pm 5.01e-03$)	1.897e-02 ($\pm 2.22e-02$)+	-3.810e-03 ($\pm 5.01e-03$)	1.897e-02 ($\pm 2.22e-02$)+									
c_0	1.329e+02 ($\pm 4.99e+00$)***	2.04	0.48	-1.817e+01 ($\pm 1.01e+01$)**	4.72	0.85	1.329e+02 ($\pm 4.99e+00$)***	2.04 (1.38)	0.48 (0.21)	-1.817e+01 ($\pm 1.01e+01$)**	4.72 (2.14)	0.85 (0.35)	DR5A [23, 151] (15)
c_1	5.708e+00 ($\pm 1.98e-01$)***			2.189e+01 ($\pm 2.01e+00$)***			5.708e+00 ($\pm 1.98e-01$)***			2.189e+01 ($\pm 2.01e+00$)***			
c_2	-6.890e-01 ($\pm 2.38e-01$)***			-1.290e+00 ($\pm 6.22e-01$)**			-6.890e-01 ($\pm 2.38e-01$)***			-1.290e+00 ($\pm 6.22e-01$)**			
c_3	-2.747e-02 ($\pm 4.10e-03$)***			-1.962e-01 ($\pm 5.51e-02$)***			-2.747e-02 ($\pm 4.10e-03$)***			-1.962e-01 ($\pm 5.51e-02$)***			
c_4	5.757e-02 ($\pm 4.75e-03$)***			1.443e-01 ($\pm 1.93e-01$)			5.757e-02 ($\pm 4.75e-03$)***			1.443e-01 ($\pm 1.93e-01$)			
c_5	-5.910e-03 ($\pm 2.63e-03$)***	1.406e-02 ($\pm 1.24e-02$)*	-5.910e-03 ($\pm 2.63e-03$)***	1.406e-02 ($\pm 1.24e-02$)*									
c_0	1.316e+02 ($\pm 5.93e+00$)***	2.52	0.57	-1.580e+01 ($\pm 1.16e+01$)*	4.93	0.98	1.316e+02 ($\pm 5.93e+00$)***	2.52 (1.25)	0.57 (0.26)	-1.580e+01 ($\pm 1.16e+01$)*	4.93 (1.63)	0.98 (0.43)	ARM71a [23, 147] (15)
c_1	5.652e+00 ($\pm 2.35e-01$)***			2.190e+01 ($\pm 2.36e+00$)***			5.652e+00 ($\pm 2.35e-01$)***			2.190e+01 ($\pm 2.36e+00$)***			
c_2	-7.848e-01 ($\pm 2.83e-01$)***			-1.428e+00 ($\pm 7.30e-01$)**			-7.848e-01 ($\pm 2.83e-01$)***			-1.428e+00 ($\pm 7.30e-01$)**			
c_3	-2.836e-02 ($\pm 4.87e-03$)***			-2.097e-01 ($\pm 6.65e-02$)***			-2.836e-02 ($\pm 4.87e-03$)***			-2.097e-01 ($\pm 6.65e-02$)***			
c_4	5.795e-02 ($\pm 5.64e-03$)***			1.636e-01 ($\pm 2.35e-01$)			5.795e-02 ($\pm 5.64e-03$)***			1.636e-01 ($\pm 2.35e-01$)			
c_5	-4.531e-03 ($\pm 3.13e-03$)**	1.825e-02 ($\pm 1.49e-02$)*	-4.531e-03 ($\pm 3.13e-03$)**	1.825e-02 ($\pm 1.49e-02$)*									
c_0	1.415e+02 ($\pm 3.85e+00$)***	6.55	1.51	-2.416e+01 ($\pm 1.41e+01$)**	8.78	1.52	1.375e+02 ($\pm 1.47e+01$)***	7.19 (3.29)	1.48 (0.45)	-1.933e+01 ($\pm 1.81e+01$)*	7.37 (5.73)	1.46 (0.62)	D2Y60 [25, 147] (17)
c_1	5.983e+00 ($\pm 4.51e-01$)***			2.993e+01 ($\pm 1.88e+00$)***			5.917e+00 ($\pm 5.21e-01$)***			2.817e+01 ($\pm 4.44e+00$)***			
c_2	-1.258e+00 ($\pm 8.43e-02$)***			-1.920e+00 ($\pm 1.14e+00$)**			-1.056e+00 ($\pm 7.11e-01$)**			-1.974e+00 ($\pm 1.16e+00$)**			
c_3	-3.242e-02 ($\pm 9.56e-03$)***			-3.040e-01 ($\pm 9.00e-02$)**			-3.103e-02 ($\pm 1.10e-02$)***			-3.391e-01 ($\pm 1.21e-01$)***			
c_4	5.958e-02 ($\pm 1.32e-02$)***						5.771e-02 ($\pm 1.52e-02$)***			2.148e-01 ($\pm 4.91e-01$)			
c_5		2.951e-02 ($\pm 2.53e-02$)*	-2.234e-03 ($\pm 7.79e-03$)	3.524e-02 ($\pm 2.88e-02$)*									
c_0	1.179e+02 ($\pm 2.13e+00$)***	15.45	1.16	-1.346e+01 ($\pm 9.14e+00$)**	13.19	1.19	1.123e+02 ($\pm 2.02e+01$)***	10.26 (2.88)	1.08 (0.44)	-1.582e+01 ($\pm 1.32e+01$)*	13.09 (5.39)	1.16 (0.61)	R32 [18, 144] (15)
c_1	4.419e+00 ($\pm 1.11e-01$)***			2.177e+01 ($\pm 2.26e+00$)***			4.090e+00 ($\pm 7.20e-01$)***			2.144e+01 ($\pm 2.72e+00$)***			
c_2				-2.101e+00 ($\pm 1.51e-01$)***			2.779e-01 ($\pm 9.74e-01$)			-1.825e+00 ($\pm 9.03e-01$)**			
c_3							7.716e-03 ($\pm 1.67e-02$)			2.191e-02 ($\pm 1.25e-01$)			
c_4	3.515e-02 ($\pm 7.61e-03$)***			-2.891e-01 ($\pm 1.45e-01$)**			3.165e-02 ($\pm 1.08e-02$)***			-3.034e-01 ($\pm 2.25e-01$)*			
c_5	-1.574e-02 ($\pm 1.07e-03$)***		-1.904e-02 ($\pm 1.13e-02$)**	-8.210e-03 ($\pm 2.92e-02$)									

^a $p < 0.1$, ^{*} $p < 0.05$, ^{**} $p < 0.01$, ^{***} $p < 0.001$; Confidence interval of 95% for regression coefficients.

^bTemperatures (K).

^cPressures (bar).

^dThe values in brackets are the errors for the full AHRI polynomial (Temperature and pressure domain).

dataset to perform a detailed analysis. Therefore, one of the scroll compressors already analyzed in Marchante-Avellaneda et al. (2023) has been selected to analyze the selection of optimal samples for the characterization of the specific energy consumption. This compressor is the ZS21KAE-PFV (Shrestha et al., 2013), with a dataset of about 60 points for the same suction temperature and refrigerant (R404A and SH = 11 K). As previously shown, the response surfaces for the specific energy consumption are very similar for both compressor typologies (scroll and reciprocating), also obtaining similar results in the case of the mass flow rate. Therefore, the conclusions obtained from the analysis of this massive dataset are easily extrapolated to reciprocating compressors.

Regarding the type of experimental design to be used, the model proposed in this work for the specific energy consumption is adjusted using nonlinear regression tools. In Marchante-Avellaneda et al. (2023) linear models selected allowed using Optimal Designs (OD) methodologies. However, OD methodologies can only be used with purely linear

models in its terms which is not the current case. That is why, this work has selected another type of design known as Cluster Designs (CD) and other typology, the Polygonal Designs (PD) (Aute et al., 2015). Both typologies are based on the automatic grouping of points in clusters, considering their location in the experimental domain, and performing the experimental sample by selecting the centroid of each cluster. The main objective will be to obtain an experimental sample homogeneously distributed over the compressor envelope. Thus, the Polygonal Design differs from the pure Cluster Design in the first manual selection of the polygon vertexes defining the compressor envelope and completing the remaining points by grouping them by clusters.

Based on the results of both methodologies, the authors have selected the Polygonal Designs as a proper methodology for compressor characterization by using non-linear correlations. It has the advantage of completely covering the experimental domain, regardless of the number of points to be included in the design, which, in the case of cluster design, compact samples tend to move away from the envelope

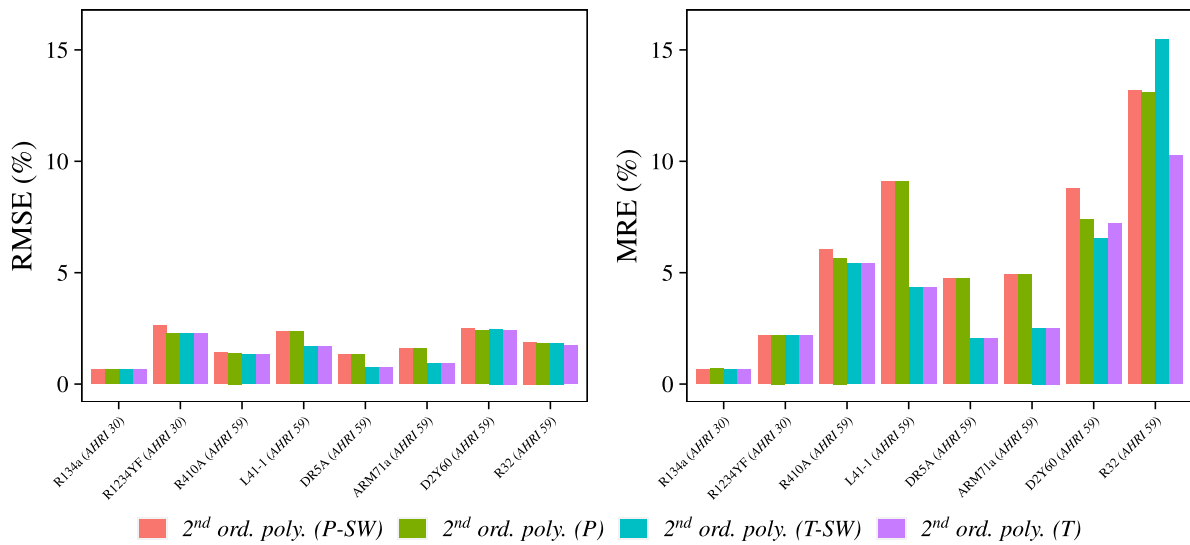


Fig. 11. Mass flow rate prediction errors (AHRI 30, 59).

edges. Moreover, the Polygonal Design includes the points located at the vertexes of the envelope in the first step. Considering that during the characterization of a compressor it is necessary to determine its working area, this type of points are in most cases necessary to test in order to obtain the working limits. Selecting as an example three samples of 7, 9, and 11 tests, Fig. 12 includes the samples generated by the Polygonal Design. The automatic selection has been performed by the open-source programming language R and the *k-means* algorithm from base package *stats*.

As can be observed in Fig. 12, the Polygonal design obtains homogeneously distributed samples over the entire compressor envelope. Once the location of the points has been obtained, Table 7 shows the model fit for of the specific energy consumption and mass flow rate. In the case of mass flow the proposed model has been the one proposed in Marchante-Avellaneda et al. (2023) (Eq. (11)) due to the greater simplicity of the response surface in scroll compressors.

$$\dot{m} = c_0 + c_1 P_e + c_2 P_c + c_3 P_e P_c \tag{11}$$

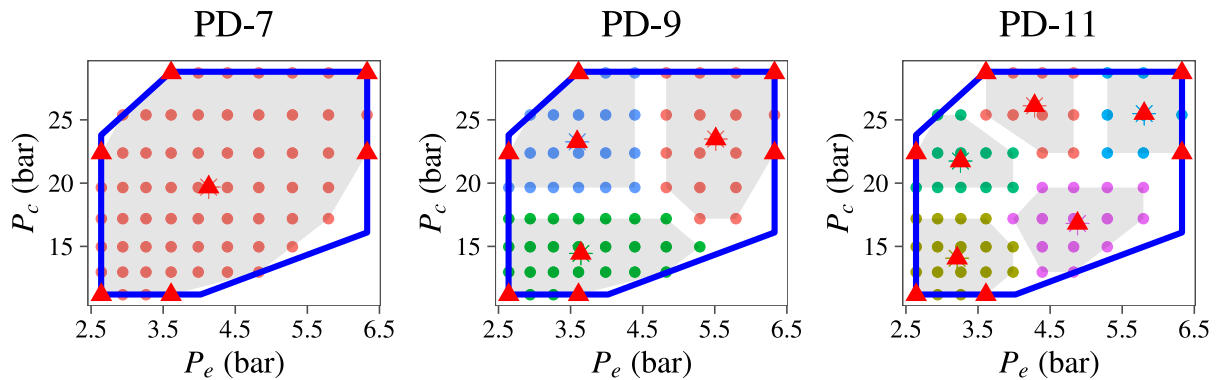


Fig. 12. Polygonal Design (7, 9, 11 test points). AHRI 21 R404A.

Table 7
Regression model adjusted with PD sample, 9 tests (AHRI 21 R404A).

	All points ^c		Sample OD (9 test points) ^c	
	\dot{W}_{esp} (kJ/kg)	\dot{m} (kg/h)	\dot{W}_{esp} (kJ/kg)	\dot{m} (kg/h)
c_0, z_c	-6.117e+00 ($\pm 6.01e-01$)***	-4.720e+00 ($\pm 2.29e+00$)***	-6.417e+00 ($\pm 4.68e+00$) ^a	-2.285e+00 ($\pm 9.04e+00$)
c_1, z_e	-6.089e-01 ($\pm 1.05e-01$)***	5.332e+01 ($\pm 5.70e-01$)***	-6.221e-01 ($\pm 9.27e-01$)	5.245e+01 ($\pm 2.78e+00$)***
c_2, k_0	-2.652e+00 ($\pm 1.38e+00$)***	-2.385e-01 ($\pm 1.13e-01$)***	-2.135e+00 ($\pm 1.16e+01$)	-3.305e-01 ($\pm 3.97e-01$) ^a
c_3, k_1	1.013e+01 ($\pm 2.59e-01$)***	-1.156e-01 ($\pm 2.67e-02$)***	1.002e+01 ($\pm 2.39e+00$)***	-8.423e-02 ($\pm 1.17e-01$)
Num.Obs.	191	63	9	9
RMSE (W, kg/h)	24.070	0.532	30.236 (17.686 ^d)	0.698 (0.917 ^d)
MRE (%)	2.845	0.850	3.048 (2.640 ^d)	0.968 (1.119 ^d)
Range (W, kg/h)	[1856, 4172]	[124, 308]	[1856, 4172]	[124, 308]

^a+p < 0.1, *p < 0.05, **p < 0.01, ***p < 0.001.

^bPressure (bar).

^cModels: Eq. (8) (\dot{W}_{esp}) and Eq. (11) (\dot{m}).

^dMRE and RMSE for the original AHRI polynomial fitted with 11 experimental points.

Table 7 also presents (in brackets) the Root Mean Square Error (RMSE) and the Maximum Relative Error (MRE) values for the original AHRI polynomial when taking into account 11 test points. This table reveals that 9 experimental tests are the best balance between sample size and model fitting accuracy.

Suppose we compare the polynomial coefficients and the prediction errors for the model adjusted with all the experimental tests. In that case, we will see that the variations in the polynomial coefficients, the RMSE, and MRE based on the adjustment comprising 9 data points have almost reached the same value. Therefore, this sample size is a suitable number of tests. In addition, through observing the MRE and RMSE values in brackets, one can conclude that the fitting of the AHRI polynomial does not enhance the accuracy and merely increases the prediction error in the mass flow rate.

Finally, it is vital to note the regression adjustment procedure employed. Since the experimental design selected includes points at the boundaries of the compressor working area, it is crucial to consider the experimental measurement error. Notably, this experimental uncertainty is more pronounced at these boundary points. For this purpose, the Inverse-Variance Weighting (IVW) has been selected instead of the classical Ordinary Least Squares (OLS) adjustment. Therefore, the weighted regression procedure selects a vector of weights for the adjustment. This vector is calculated as the inverse of the square of the combined standard uncertainty for each observation (Taylor and Kuyatt, 1994).

7. Conclusions

This paper presents a comprehensive examination of mass flow rate and energy consumption modeling in reciprocating compressors selecting the empirical model approach. The analysis covered all reciprocating compressors published in the reports from the “Low-GWP Alternative Refrigerants Evaluation program”. The main conclusions from this work are summarized below:

- Similar trends have been obtained from the analysis of the response surface of the compressor efficiency to the previous ones reported in Marchante-Avellaneda et al. (2023) for scroll compressors. The corresponding response surface depends on the suction conditions with a complex shape.
- The energy consumption response surfaces show the greatest difference in their behavior between technologies (scroll/reciprocating). These are more straightforward in scroll compressors and can be more complex in reciprocating compressors. This complexity depends on the operating range and may require polynomials with a higher number of terms. Therefore it may be justified to use third-degree polynomials as proposed by the current compressor characterization standard (AHRI 540, 2020).
- Once the response surfaces for the energy consumption in reciprocating compressors were analyzed, it was possible to identify two different trends. The first one includes a simpler response surface, practically a plane, depending on the evaporation conditions for L/M-BP compressors. The second one shows a more complex response surface with higher complexity and curvature for HBP compressors, which depends on condensing and evaporating conditions.
- In general, using a second-degree polynomial for characterizing scroll compressors – and probably rotary compressors – does not result in higher prediction accuracy due to overfitting. This is not true for reciprocating compressors, where the greater complexity of the response surfaces may justify the use of third-degree polynomials.
- Contrary to scroll compressors, the use of the original 10-term AHRI polynomial for reciprocating compressor characterization is justified. The authors have confirmed that automatic-term-reduction methodologies can be used to simplify the final polynomial model, eliminating any possible collinearity effects when

the response surface is simpler. Alternatively, other strategies, such as the Thin-Plate-Spline regression model, may be used to generate the compressor maps with a smooth interpolation. Nevertheless, it has been probed that the expressions obtained with these techniques depend on the compressor and refrigerant.

- The compressor characterization in terms of the specific energy consumption significantly reduces the number of the parameters required by the functional in order to estimate the energy consumption and supply a general function depending only on 4 parameters (or 5/6 if we want to increase the prediction accuracy by increasing the degree of the polynomial) and unify the behavior for the two compressor technologies analyzed. Therefore, the model becomes more stable by minimizing possible problems of extrapolation or interpolation to areas of the map not covered by the experimental sample used for the adjustment. Moreover, the significant reduction in the number of terms of the polynomial allows defining more compact experimental matrices, thus reducing the experimental costs and time.
- The mass flow rate can be reproduced using second-order polynomials, so using the third-order AHRI polynomials is not justified for this variable in reciprocating compressors.
- The prediction errors for approaches based on saturation temperature or pressure are in the same range. However, if pressure variables are selected, the compressor consumption model parameters are more refrigerant-independent for a specific compressor.
- Even though the guidelines included in the standard do not indicate anything in terms of picking out samples, Polygonal Design technique can be employed to pick the experimental samples and carry out the experimental test matrix in the compressor's envelope. In order to enhance the model's precision, 9 points is an appropriate sample size for modeling the mass flow rate and the specific energy consumption.

Considering all the above, we can state that the search for a general polynomial expression capable of accurately characterizing the performance in reciprocating compressors results in using third-order polynomials, as reported in the current standard (AHRI 540, 2020). However, in the case of the scroll compressor, it results in overfitting the model, as reported by Marchante-Avellaneda et al. (2023). Consequently, if the model predicts in areas not covered by the fitting data, it is possible to obtain significant extrapolation and interpolation errors. The latter may lead us to think that the models, defined years ago in the standard, were proposed in a context where, in those years, the predominant technology was the reciprocating compressor and, over the years, its application has been extending to other typologies, such as scroll compressors.

Declaration of competing interest

The authors declare that they have no known competing financial interests or personal relationships that could have appeared to influence the work reported in this paper.

Acknowledgments

The present work has been supported by the project “DESCARBONIZACIÓN DE EDIFICIOS E INDUSTRIAS CON SISTEMAS HÍBRIDOS DE BOMBA DE CALOR”, funded by the “Ministerio de Ciencia e Innovación”, MCIN, Spain, with code number: PID2020-115665RB-I00 and by the “Ministerio de Educación, Cultura y Deporte”, MECD, Spain, inside the program “Formación de Profesorado Universitario (FPU15/03476)”. This research used resources at the Building Technologies Research and Integration Center, a DOE Office of Science User Facility operated by the Oak Ridge National Laboratory of USA.

Appendix A. Supplementary data

Supplementary material related to this article can be found online at <https://doi.org/10.1016/j.ijrefrig.2023.06.002>.

References

- AHRI 540, 2020. AHRI 540 - standard for performance rating of positive displacement refrigerant compressors and compressor units. URL: <https://www.ahrinet.org/search-standards/ahri-540-si-i-p-performance-rating-positive-displacement-refrigerant-compressors-and-compressor>.
- ANSI/ASHRAE Standard 34, 2019. Designation and Safety Classification of Refrigerants. Technical Report, American Society of Heating and Air-Conditioning Engineers, URL: <https://www.ashrae.org/technical-resources/standards-and-guidelines/ashrae-refrigerant-designations>.
- Aute, V., Martin, C., 2016. A comprehensive evaluation of regression uncertainty and the effect of sample size on the AHRI-540 method of compressor performance representation. In: International Refrigeration and Air Conditioning Conference. Paper 2457. Purdue University, West Lafayette, Indiana, URL: <https://docs.lib.purdue.edu/cgi/viewcontent.cgi?article=3456&context=icec>.
- Aute, V., Martin, C., Radermacher, R., 2015. AHRI Project 8013 : A Study of Methods to Represent Compressor Performance Data over an Operating Envelope Based on a Finite Set of Test Data. Air-Conditioning, Heating, and Refrigeration Institute, URL: https://www.ahrinet.org/sites/default/files/2022-07/AHRI-8013_Final_Report.pdf.
- Borges Ribeiro, G., Marchi Di Gennaro, G., 2013a. TEST REPORT #17. Compressor Calorimeter Test of Refrigerants R-22 and R-1270. Technical Report, Embraco.
- Borges Ribeiro, G., Marchi Di Gennaro, G., 2013b. TEST REPORT #18. Compressor Calorimeter Test of Refrigerants R-134a, N-13a and ARM-42a. Technical Report, Embraco.
- Boscan, M., Sanchez, J., 2015. TEST REPORT #51. Compressor Calorimeter Test of Refrigerant Blend DR-33 (R449A) in a R-404A Reciprocating Compressor. Technical Report, Bitzer US.
- Bourdouxhe, J.P., Grodent, M., Silva, K.L., Lebrun, J.J., Saavedra, C., 1994. A toolkit for primary HVAC system energy calculation. Part 2: Reciprocating chiller models. In: 1994 Annual Conference, Orlando, FL, Vol.100. ASHRAE Trans., 1994, Part 2, Paper OR-94-9.
- Cheung, H., Wang, S., 2018. A comparison of the effect of empirical and physical modeling approaches to extrapolation capability of compressor models by uncertainty analysis: A case study with common semi-empirical compressor mass flow rate models. *Int. J. Refrig.* 86, 331–343. <http://dx.doi.org/10.1016/j.ijrefrig.2017.11.020>.
- Chua, K.J., Chou, S.K., Yang, W.M., 2010. Advances in heat pump systems: A review. *Appl. Energy* 87 (12), 3611–3624. <http://dx.doi.org/10.1016/j.apenergy.2010.06.014>.
- Corberan, J.M., Gonzalez, J., Urchueguia, J., Calas, A., 2000. Modelling of refrigeration piston compressors. In: 15th International Compressor Engineering Conference at Purdue. Paper 1436. Purdue University, URL: <https://docs.lib.purdue.edu/icec/1436/>.
- Core Team, R., 2022. R: A language and environment for statistical computing.
- Dabiri, A.E., Rice, C.K., 1981. A compressor simulation model with corrections for the level of suction gas superheat. In: 1981 Annual Conference, Cincinnati, OH, Vol. 87. ASHRAE Trans., 1981, Part 2, Paper CI-81-6.
- Fox, J., 2022. Rcmdrmisc: R commander miscellaneous functions. R package version 2.7-2.
- Green, P.J., Silverman, B.W., 1993. Nonparametric Regression and Generalized Linear Models. Chapman & Hall.
- Guth, T., Atakan, B., 2023. Semi-empirical model of a variable speed scroll compressor for R-290 with the focus on compressor efficiencies and transferability. *Int. J. Refrig.* 146 (October 2022), 483–499. <http://dx.doi.org/10.1016/j.ijrefrig.2022.10.024>.
- Lemmon, E.W., Bell, I.H., Huber, M.L., McLinden, M.O., 2018. NIST Standard Reference Database 23: Reference Fluid Thermodynamic and Transport Properties-REFPROP, Version 10.0. National Institute of Standards and Technology, <http://dx.doi.org/10.18434/T4/1502528>, URL: <https://www.nist.gov/srd/refprop>.
- Lenz, J.R., Shrestha, 2016. TEST REPORT #59. Compressor Calorimeter Test of Refrigerants L41-1, DR-5A, ARM-71a, D2Y-60 and R-32 in a R-410A Reciprocating Piston Compressor. Technical Report, Bristol compressor & Oak Ridge National Laboratory.
- Mackensen, A., Klein, S.A., Reindl, D.T., 2002. Characterization of refrigeration system compressor performance. In: International Refrigeration and Air Conditioning Conference at Purdue. Paper 567. Purdue University, URL: <https://docs.lib.purdue.edu/iracc/567/>.
- Marchante-Avellaneda, J., Corberan, J.M., Navarro-Peris, E., Shrestha, S.S., 2023. A critical analysis of the AHRI polynomials for scroll compressor characterization. *Appl. Therm. Eng.* 219, 119432. <http://dx.doi.org/10.1016/J.APPLTHERMALENG.2022.119432>, URL: <https://linkinghub.elsevier.com/retrieve/pii/S135943112201362X>.
- Marchante-Avellaneda, J., Navarro-Peris, E., Corberán, J.M., Shrestha, S.S., 2022. A critical analysis of the characterization of reciprocating compressors energy consumption. In: 26th International Compressor Engineering Conference at Purdue. Paper 2757. Purdue University, West Lafayette, Indiana, URL: <https://docs.lib.purdue.edu/icec/2757/>.
- Navarro, E., Granryd, E., Urchueguía, J.F., Corberán, J.M., 2007. A phenomenological model for analyzing reciprocating compressors. *Int. J. Refrig.* 30 (7), 1254–1265. <http://dx.doi.org/10.1016/j.ijrefrig.2007.02.006>.
- Navarro-Peris, E., Corberán, J.M., Falco, L., Martínez-Galván, I.O., 2013. New non-dimensional performance parameters for the characterization of refrigeration compressors. *Int. J. Refrig.* 36 (7), 1951–1964. <http://dx.doi.org/10.1016/j.ijrefrig.2013.07.007>.
- Pérouffe, L., Renevier, G., 2016a. TEST REPORT #64. Compressor Calorimeter Test of Refrigerant DR-7 (R-454A) in a R-404A Reciprocating Compressors. Technical Report, Tecumseh Products Company.
- Pérouffe, L., Renevier, G., 2016b. TEST REPORT #67. Compressor Calorimeter Test of Refrigerant ARM-25 in a R-404A Reciprocating Compressors. Technical Report, Tecumseh Products Company.
- Pérouffe, L., Renevier, G., 2016c. TEST REPORT #69. Compressor Calorimeter Test of Refrigerant ARM-20b in a R-404A Reciprocating Compressors. Technical Report, Tecumseh Products Company.
- Pierre, B., 1982. Kylteknik, Allmän Kurs. Mekanisk värmeteri och kylteknik, KTH, Stockholm, Sweden.
- Popovic, P., Shapiro, H.N., 1995. A semi-empirical method for modeling a reciprocating compressor in refrigeration systems. In: 1995 Annual Conference, San Diego, CA, Vol. 101. ASHRAE Trans., 1995, Part 2, Paper 3912.
- Rajendran, R., Nicholson, A., 2014a. TEST REPORT #35. Compressor Calorimeter Test of Refrigerant DR-7 in a R-404A Reciprocating Compressor. Technical Report, Emerson Climate Technologies.
- Rajendran, R., Nicholson, A., 2014b. TEST REPORT #37. Compressor Calorimeter Test of Refrigerant L-40 in a R-404A Reciprocating Compressor. Technical Report, Emerson Climate Technologies.
- Rasmussen, B.D., Jakobsen, A., 2000. Review of compressor models and performance characterizing variables. In: 15th International Compressor Engineering Conference at Purdue. Paper 1429. Purdue University, URL: <https://docs.lib.purdue.edu/icec/1429/>.
- Roskosch, D., Venzik, V., Atakan, B., 2017. Thermodynamic model for reciprocating compressors with the focus on fluid dependent efficiencies. *Int. J. Refrig.* 84, 104–116. <http://dx.doi.org/10.1016/j.ijrefrig.2017.08.011>.
- Sedliak, J., 2013a. TEST REPORT #28. Compressor Calorimeter Test of R404A Alternative Refrigerant L-40 in Reciprocating Compressors. Technical Report, Embraco.
- Sedliak, J., 2013b. TEST REPORT #29. Compressor Calorimeter Test of R404A Alternative Refrigerant DR-7 in Reciprocating Compressors. Technical Report, Embraco.
- Sedliak, J., 2013c. TEST REPORT #30. Compressor Calorimeter Test of R134a Alternative Refrigerant R-1234yf in Reciprocating Compressors. Technical Report, Embraco.
- Sedliak, J., 2015a. TEST REPORT #49. Compressor Calorimeter Test of Refrigerant Blend HDR110 in a R-404A Reciprocating Compressor. Technical Report, Embraco.
- Sedliak, J., 2015b. TEST REPORT #50. Compressor Calorimeter Test of Refrigerant Blend DR-3 in a R-404A Reciprocating Compressor. Technical Report, Embraco.
- Shao, S., Li, X., Shi, W., Chen, H., 2004. Performance representation of variable-speed compressor for inverter air conditioners based on experimental data. *Int. J. Refrig.* 27 (8), 805–815. <http://dx.doi.org/10.1016/j.ijrefrig.2004.02.008>.
- Shrestha, S., Sharma, V., Abdelaziz, O., 2013. TEST REPORT #21. Compressor Calorimeter Test of R-404A Alternatives ARM-31a, D2Y-65, L-40, and R-32/R-134a (50/50). Technical Report, Oak Ridge National Laboratory.
- Taylor, B.N., Kuyatt, C.E., 1994. Guidelines for Evaluating and Expressing the Uncertainty of NIST Measurement Results. Technical Report, National Bureau of Standards, Gaithersburg, MD, <http://dx.doi.org/10.6028/NIST.TN.1297>.
- Vering, C., Stopp, D., Klebig, T., Venzik, V., Müller, D., 2021. Optimal designed experiments for reliable model calibration of a fixed-speed scroll compressor with R410A and R32. In: IOP Conference Series: Materials Science and Engineering, Vol. 1180. 012032. <http://dx.doi.org/10.1088/1757-899x/1180/1/012032>.
- Winandy, E., Saavedra O., C., Lebrun, J., 2002. Simplified modelling of an open-type reciprocating compressor. *Int. J. Therm. Sci.* 41 (2), 183–192. [http://dx.doi.org/10.1016/S1290-0729\(01\)01296-0](http://dx.doi.org/10.1016/S1290-0729(01)01296-0).